

Dear editor and referee#1,

Thank you very much for your time and attentions on this work. The constructive comments and suggestions are very useful to improve our manuscript. Following are point-by-point responses to referee #1's comments. All the line numbers mentioned in responses are referred to the manuscript with changes marked.

(1) From a general point of view, I would suggest the authors to maybe underline more efficiently the novelty of the study and its interest. Maybe that authors need, to do so, to modify the section of introduction. For instance, authors need to revise the aims of the study based on the results and conclusions. At least, it is necessary to highlight the different aerosol effects on CG lightning between in the plateau and basin regions of Sichuan, Southwest China.

**Reply:** We have revised the introduction and highlighted the aim of the study. “There are significant geographical and environmental differences between the western Sichuan plateau and the eastern Sichuan basin. The thermal conditions of the western Sichuan Plateau are obviously weaker than those of the Sichuan Basin (Qie et al., 2003), and the aerosol concentration in the plateau is also significantly lower than that in the basin (Ning et al., 2018a). Previous studies (Yuan et al., 2011; Wang et al., 2011; Yang et al., 2013; Yang and Li, 2014; Fan et al., 2015) have suggested that aerosol effects on lightning activity differ significantly due to differences in topography and aerosol. The purpose of this study is to investigate any similarities and differences in the effects of aerosols on lightning activity in the context of different topography and aerosol concentrations between the Western Sichuan Plateau and Sichuan Basin.” The details can be seen L136-145 of the revised manuscript.

(2) Both Lines 120-126 in the introduction section and Lines 138-143 in the Data and methodology section describe the complex topography around Sichuan province. Thus, I suggest that the authors move the contents of Lines 138-143 to the introduction section and rewrite the parts related to the complex topography around Sichuan Basin.

**Reply:** We have moved this sentence to the introduction section and rewrote the

parts related to the complex topography around Sichuan Basin. The details can be seen L125-130 of the revised manuscript.

(3) Lines 128-132: “Previous studies have suggested that ....” belongs to future research plane and not to the research goal of this study, which is not suitable to appear in the section of introduction. These sentences should be moved to the discussion or conclusion section to indicate the limitations of this article that need to be solved in future research.

**Reply:** We have moved this sentence to the conclusion section to indicate the limitation of current study and the potential of the future study. The details can be seen L703-708 of the revised manuscript.

(4) Lines 275-279: the correlation between aerosol loading and lightning is negative in the basin region but is positive correlation in the plateau region. According to the above correlation coefficients, the authors concluded that aerosols stimulate lightning in the plateau region, but suppress lightning in the basin region. I think this conclusion is unconvincing. I thus suggest that the authors need to provide more sufficient evidence.

**Reply:** To further verify the stimulation and inhibition of aerosols on lightning activity and eliminate the interference of seasonality on the effects of aerosols on lightning, Pearson correlation coefficients between anomalies of total AOD and CG lightning and anomalies of sulfate AOD and CG lightning were implemented. As can be seen from the comparison between Fig. 3 and Fig. 4, the correlation coefficients between anomalies of AOD and lightning are significantly lower than those between AOD and lightning. While in an overall view, there is still a positive correlation between aerosols and lightning in the plateau region, and a negative correlation between aerosols and lightning in the basin region, especially for sulfate aerosols. This further verifies that aerosols have the potential to stimulate lightning activity in the plateau region and inhibit lightning activity in the basin region. The specific physical relationship will be further discussed below. The above discussion and the following figure as Figure 4 have been added to the revised manuscript. The details can be seen L344-364 of the revised

manuscript.

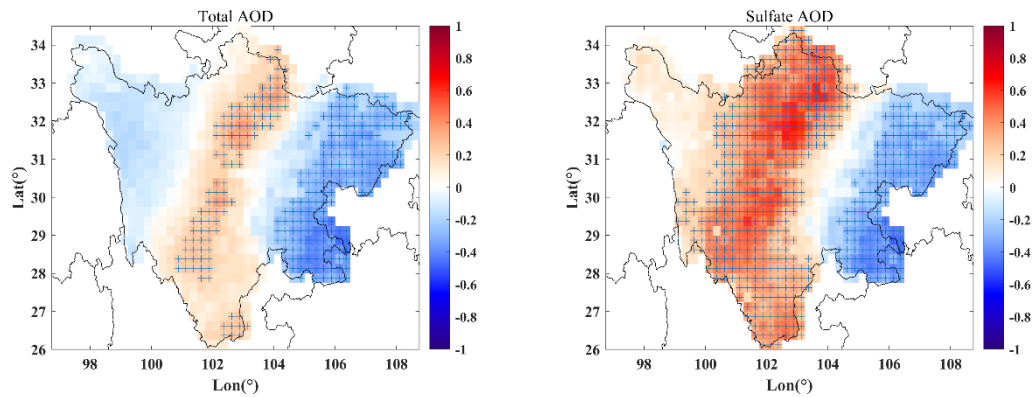


**Figure 4.** Pearson correlation coefficients between anomalies of total AOD and CG lightning (left panel) and anomalies of sulfate AOD and CG lightning (right panel) based on monthly data from 2005 to 2017. Crosses in the figure indicate grid boxes that have passed the 90% significance test.

(5) Lines 288-289: ‘Since sulfate AOD accounts for more than 80% of the total AOD in Sichuan, ...’, while as shown in Figure 2, sulfate AOD accounts for about 60-80% of the total AOD over the basin region and 40-55% of the total AOD over the plateau region. Please check it.

**Reply:** It has been revised.

(6) I suggest that the authors need to perform a significance test on the curve fitting results in Figure 4.

**Reply:** We have carried out significance test on the curve fitting results by using F-test method, and the P value of both curves is less than 0.001, indicating that the curve fitting results are significant. We have redrawn Figure 4 as Figure 5, marked the P value in the figure, and made modifications in the revised manuscript. The details can be seen L384-387 of the revised manuscript.

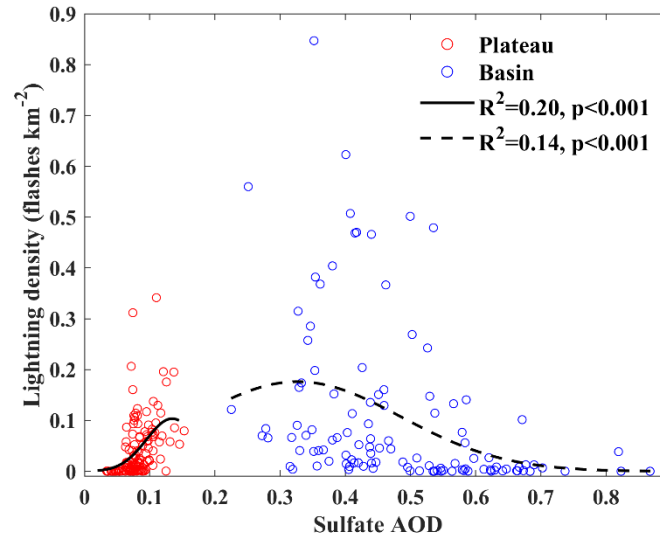


**Figure 5.** CG lightning density as a function of sulfate AOD over the basin (blue circles) and plateau (red circles) regions. Exponential-fit curves are shown, and coefficients of determination ( $R^2$ ) and p values are given.

(7) Lines 442-445: “From the joint ..., an increase in CAPE inhibits the vertical wind shear in the lower to middle troposphere...” Why does an increase in CAPE inhibits the vertical wind shear?

**Reply:** CAPE is directly related to the upward movement, and CAPE can even be used to estimate the maximum updraft velocity (Molinari et al., 2012). Strong upward motion is not conducive to the development of vertical wind shear. previous studies (Li et al., 2013; Sherburn et al., 2016) on the complex of strong convection and mesoscale convection also found that the environmental vertical wind shear was smaller when CAPE was larger. Relevant references have been added to the revised manuscript. The details can be seen L524 of the revised manuscript.

(8) In the sections 3.5, the multiple linear regressions of CG lighting have been developed in the plateau region (as shown in EQ.6) and in the basin region (as shown in EQ.7), respectively. However, the positive or negative values of the regression coefficients in front of each regression factor (such AOD, RH, CBH, TCIW, and TCLW) are inconsistent with the Pearson correlation coefficients between these factors and CG

lightning in Figure 3 and Figure 5. For instance, the Pearson correlation coefficients between sulfate AOD and CG lightning are opposite between in the plateau region and the basin region; while the values of the regression coefficients associated with AOD are both positive in EQ.6 and EQ.7. I suggest authors to check the above results based on the multiple linear regression and give reasonable explanations. In addition, the similar situations are also observed in EQ.9.

**Reply:** In this study, we used multiple linear regression methods to fit the lightning density in Sichuan, and the regression factors included CAPE, RH, SHEAR, CBH, TCLW, TCIW, and AOD. In order to further analyze the most prominent factor contributing to the lightning density, we use the stepwise regression method to fit the lightning density. Because different factors contributed different proportions to the lightning density, there was a discrepancy between the positive and negative values of the regression factors and the positive and negative values of the Pearson correlation coefficient. Previous study (Wang et al., 2018) also had a similar situation.

#### **Minor comments**

(1) It is better to give a table of acronym because there are many abbreviations in the manuscript.

**Reply:** The acronym table has been added in the revised manuscript. The details can be seen in L274-276 in revised manuscript.

(2) Line 123: 'diffusion' -> 'dispersion'

**Reply:** It has been revised.

(3) Lines 122-124: "The Sichuan basin is an area with high aerosol loading and with terrain ... (X. Zhang et al., 2012; L. Sun et al., 2016; Wei et al., 2019a, b)" is suggested to be changed to "The Sichuan basin is an area with high aerosol loading and with complex terrain ... (Zhang et al., 2012; Sun et al., 2016; Wei et al., 2019a, b; Ning et al., 2017, 2019)".

**Reply:** It has been revised.

(4) Line 127: 'influence' -> 'influences'

**Reply:** It has been revised.

(5) Line 176:“E. Sun et al. (2018, 2019) employed ...” ->“Sun et al. (2018, 2019) employed ...”

**Reply:** It has been revised.

(6) Line 192:“S. Lee et al. (2018) compared the ...” ->“Lee et al. (2018) compared the ...”

**Reply:** It has been revised.

(7) Line 270: ‘influenced’-> ‘affected’

**Reply:** It has been revised.

(8) Line 395: ‘over 1000’ -> ‘greater 1000’

**Reply:** It has been revised.

(9) Line 567: ‘influence’ -> ‘influences’

**Reply:** It has been revised.

(10) Line 577:‘diffusion’ -> ‘dispersion’

**Reply:** It has been revised.

#### Reference:

Fan, J., Rosenfeld, D., Yang, Y., Zhao, C., Leung, L. R. and Li, Z.: Substantial contribution of anthropogenic air pollution to catastrophic floods in Southwest China. *Geophys. Res. Lett.*, 42(14), 6066-6075, <https://doi.org/10.1002/2015GL064479>, 2015.

Li, X., Guo, X. and Fu, D.: TRMM-retrieved cloud structure and evolution of MCSs over the northern South China Sea and impacts of CAPE and vertical wind shear, *Adv. Atmos. Sci.* 30, 77–88, <https://doi.org/10.1007/s00376-012-2055-2>, 2013.

Molinari, J., Romps, D.M., Vollaro, D. and Nguyen, L.: CAPE in tropical cyclones, *J. Atmos. Sci.*, 69 (8): 2452–2463. <https://doi.org/10.1175/JAS-D-11-0254.1>, 2012.

Ning, G., Wang, S., Ma, M., Ni, C., Shang, Z., Wang, J. and Li, J.: Characteristics of air pollution in different zones of Sichuan Basin, China. *Sci. Total Environ.*, 612, 975–984, <https://doi.org/10.1016/j.scitotenv.2017.08.205>, 2018a.

Qie, X., Toumi, R., Zhou, Y. J.: Lightning activity on the central Tibetan Plateau and its response to convective available potential energy, *Chinese Science Bulletin*,

48(3), 296–299, <https://doi.org/10.1007/BF03183302>, 2003.

Sherburn, K.D., Parker, M.D., King, J.R. and Lackmann, G.M.: Composite environments of severe and nonsevere high-shear, low-CAPE convective events, *Wea. forecasting*, 31(6), 1899-1927. <https://doi.org/10.1175/WAF-D-16-0086.1>, 2016.

Wang, Q., Li, Z., Guo, J., Zhao, C. and Cribb, M.: The climate impact of aerosols on the lightning flash rate: is it detectable from long-term measurements?, *Atmos. Chem. Phys.*, 18(17), 12797–12816, <https://doi.org/10.5194/acp-18-12797-2018>, 2018.

Wang, Y., Wan, Q., Meng, W., Liao, F., Tan, H., and Zhang, R.: Long-term impacts of aerosols on precipitation and lightning over the Pearl River Delta megacity area in China. *Atmos. Chem. Phys.*, 11, 12421–12436, <https://doi.org/10.5194/acp-11-12421-2011>, 2011.

Yang, X., Yao, Z., Li, Z. and Fan, T.: Heavy air pollution suppresses summer thunderstorms in central China. *J. Atmos. Sol.-Terr. Phy.*, 95, <https://doi.org/10.1016/j.jastp.2012.12.023>, 28–40, 2013.

Yang, X., and Li, Z.: Increases in thunderstorm activity and relationships with air pollution in southeast China, *J. Geophys. Res. Atmos.*, 119, 1835–1844, <https://doi.org/10.1002/2013JD021224>, 2014.

Yuan, T., Remer, L. A., Pickering, K. E., Yun, H.: Observational evidence of aerosol enhancement of lightning activity and convective invigoration, *Geophys. Res. Lett.*, 38, L04701, <https://doi.org/10.1029/2010GL046052>, 2011.

Dear editor and referee #2,

Thank you very much for your time and attentions on this work. The constructive comments and suggestions are very useful to improve our manuscript. Following are point-by-point responses to referee #2's comments. All the line numbers mentioned in responses are referred to the manuscript with changes marked.

(1) L99-106, radiation absorption by aerosols can either suppress or enhance convection via altering CAPE depend on the heating vertical profile and the elevation where the convection initiates. Please see the discuss and the schematic of Wang et al. (2013, "New Directions: Light Absorbing Aerosols and Their Atmospheric Impacts").

**Reply:** We have added this sentence "Absorbing aerosols in the boundary layer warm the atmosphere and cool the surface, which leads to the increase of atmospheric convective inhibition energy and the rise of convection condensation level (CCL), meanwhile the absorbing aerosols also leads to the increase of convective available potential energy above CCL. Once the lifting condition overcomes the convective inhibition energy, strong convective activity will be triggered (Wang et al., 2013)." and deleted the sentence "Absorbing aerosols block solar radiation from reaching the surface through radiative effects, which tends to inhibit the development of convection." The details can be seen L97-103 of the revised manuscript.

(2) L178-179, it is not surprising to see good agreement between MERRA2-Aero and MODIS AOD, as MERRA2-Aero assimilates MODIS AOD product. Can the authors obtain the AOD from an independent satellite, such as MISR, to confirm the variability of the AOD near Sichuan?

**Reply:** Figure S1 shows the spatial distribution of AOD based on the monthly data of MEERA2 and MISR data sets from 2005 to 2017. It can be seen from Fig S1 that the AOD spatial distribution of MISR is very close to that of MERRA, but the AOD value of MISR is smaller than that of MERRA2. Wei et al. (2019) suggest that there is a good consistency between MISR and MODIS AOD products in southwest China by using multi-satellite data comparison. The details can be seen L202-208 of the revised



manuscript.

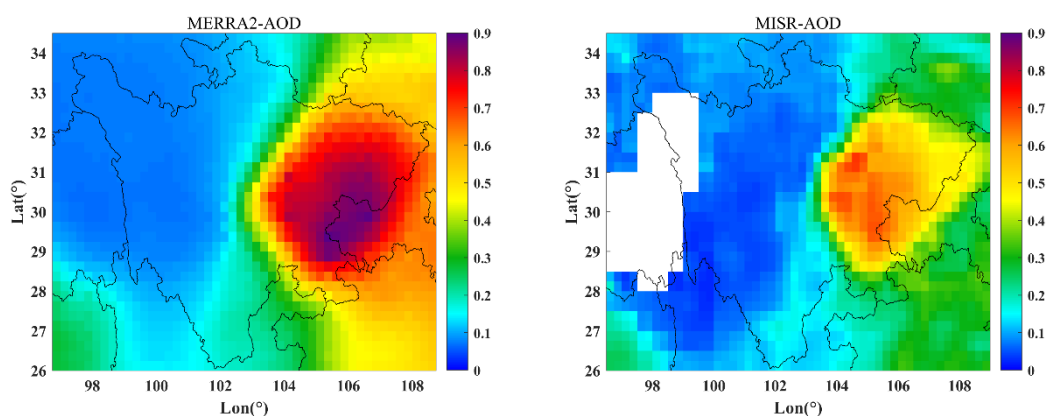


**Figure S1.** The spatial distribution of annual mean AOD based on MERRA2 and MISR data sets from 2005 to 2017

(3) The uncertainty of cloud product from ERA5 over Southwest China seems unclear. Can the author make comparison of liquid/ice content between ERA5 and MODIS?

**Reply:** Due to the low spatial resolution ( $1^{\circ}\times 1^{\circ}$ ) of MODIS monthly cloud product, we chose the cloud product of CLARA-A2 ( $0.25^{\circ}\times 0.25^{\circ}$ ) for comparison with the cloud product of ERA5. CLARA-A2 is the second edition of the Satellite Application Facility on Climate Monitoring (CM SAF) cloud, albedo, and surface radiation dataset. The CLARA-A2 record provides cloud properties, surface albedo, and surface radiation parameters derived from the Advanced Very High-Resolution Radiometer (AVHRR) sensor (Karlsson et al., 2017; Karlsson and Håkansson, 2018). Figure S2 shows the spatial distribution of liquid water path (LWP) and ice water path (IWP) based on the monthly data of ERA5 and CLARA-A2 data sets from 2005 to 2015. LWP is high in the east and low in the west of Sichuan, while LWP in ERA5 is obviously lower than that of CLARA-A2 in the northwest of Sichuan. The spatial distribution of IWP in the two data sets are close, LWPs in northwestern Sichuan are higher than that in eastern and southern Sichuan.

We compared LWPs and IWPs of CLARA-A2 and ERA5 data sets, and overall, the cloud products of the two data sets were similar. For the continuity of data, LWP and IWP in ERA5 were selected in this study. We have added the above texts to the revised manuscript and the following figure to the supplement as figure S2. The details can be seen L230-236 of the revised manuscript.

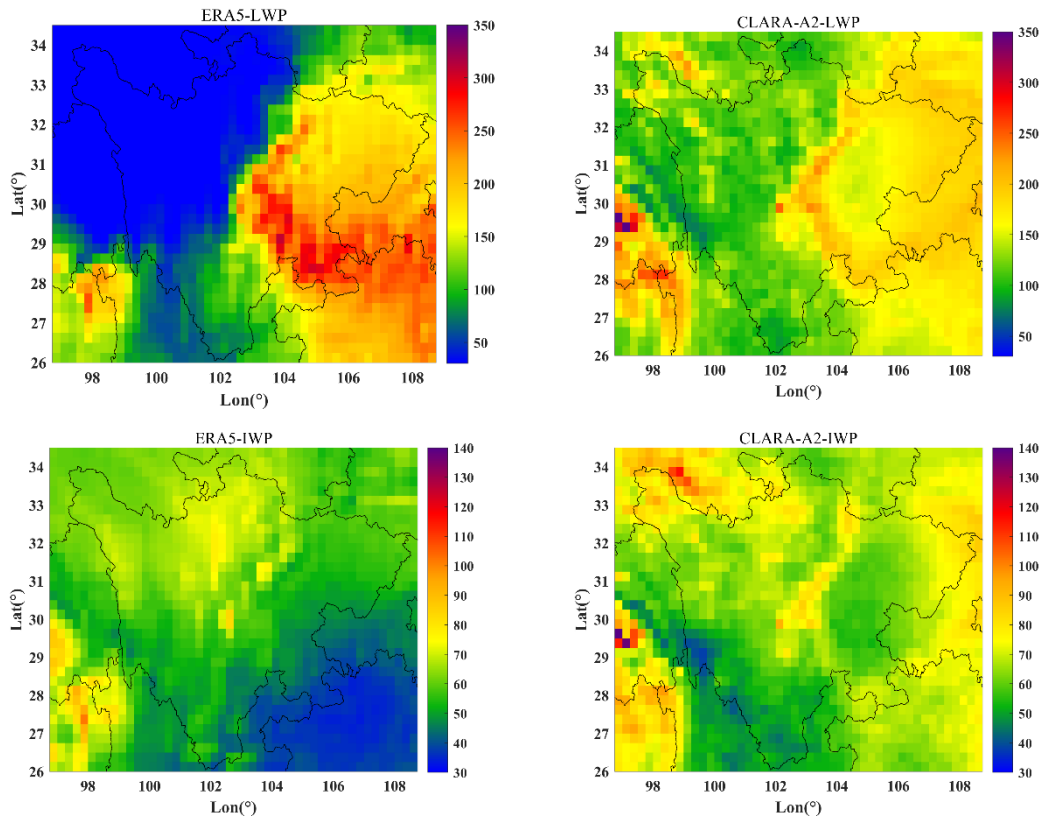


**Figure S2.** The spatial distribution of annual mean LWP and IWP based on ERA5 and CLARA-A2 data sets from 2005 to 2015

(4) Figs. 3,5-7. for the correlations between the time series of monthly mean data, do they mainly reflect the seasonality? Are they still significant if you remove the seasonality and look at anomalies (interannual variability) only?

**Reply:** To eliminate the interference of seasonality on the effects of aerosols on lightning, Pearson correlation coefficients between anomalies of total AOD and CG lightning and anomalies of sulfate AOD and CG lightning were implemented. As can be seen from the comparison between Fig. 3 and Fig. 4, the correlation coefficients between the anomalies of AOD and lightning are significantly lower than those between AOD and lightning. While in an overall view, there is still a positive correlation between aerosols and lightning in the plateau region, and a negative correlation between aerosols and lightning in the basin region, especially for sulfate aerosols. This further verifies that aerosols have the potential to stimulate lightning activity in the plateau region and inhibit lightning activity in the basin region. The specific physical relationship will be further discussed below. The above discussion and the following figure as Figure 4 have

been added to the revised manuscript. The details can be seen L344-364 of the revised manuscript.

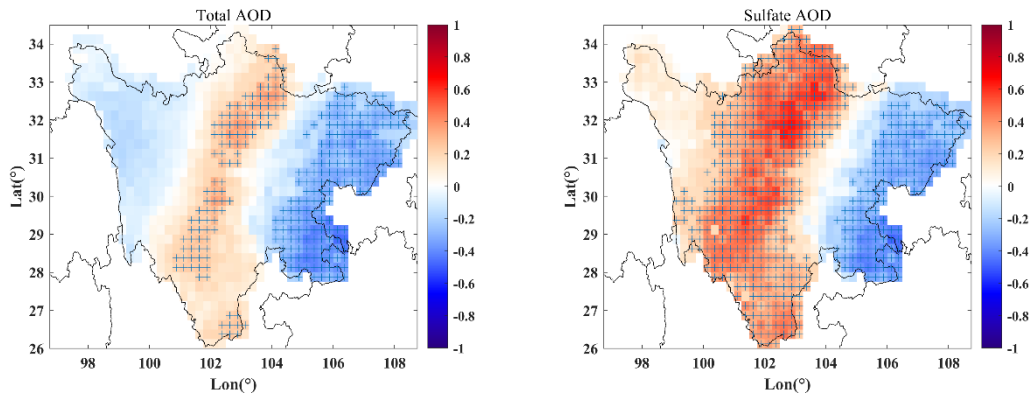


**Figure 4.** Pearson correlation coefficients between anomalies of total AOD and CG lightning (left panel) and anomalies of sulfate AOD and CG lightning (right panel) based on monthly data from 2005 to 2017. Crosses in the figure indicate grid boxes that have passed the 90% significance test.

Fig. S3 shows the correlation coefficients between the anomalies of CAPE, RH, SHEAR, CBH, TCLW, and TCIW and CG lightning. Compared with Figure 6 in the revised manuscript, the correlation coefficients are obviously smaller, especially in the basin region. The significances of the correlation between CG lightning and environmental factors are weakened, especially SHERA, CBH, and TCLW in the basin region. The above discussion has been added to the revised manuscript, and the following figure has been added to the supplement as Figure S3. The details can be seen L413-417 of the revised manuscript.

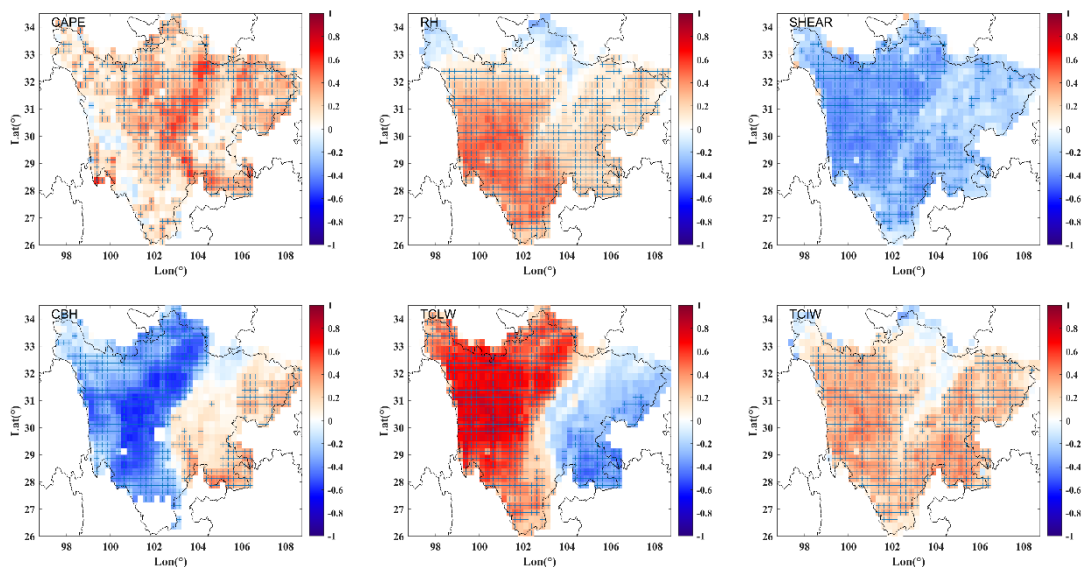


**Figure S3.** Pearson correlation coefficients between the anomalies of CAPE, RH, SHEAR, CBH, TCLW, and TCIW and CG lightning. Crosses in the figure indicate grid boxes that have passed the 95% significance test.

In the revised manuscript, we recalculated the partial correlation coefficient between meteorological factors and lightning, which is shown in Figure 7 in the revised manuscript. We used partial correlation coefficients to discuss the dependence of lightning on a meteorological factor relatively independently. The partial correlation coefficients in Figure 7 in the revised manuscript is small, while the partial correlation calculated by using the anomalies of variables is not significant.

(5) Figs, 6 and 7, how are the partial correlation coefficients calculated and how are they different from the total correlation coefficient? My understanding is the partial correlation is a measure of the dependence between two variables where the influence from other possible controlling variables (like meteorological parameters in this case) is removed. This method has been used in many previous aerosol-cloud studies (e.g. Zhao et al., 2019, “Ice nucleation by aerosols from anthropogenic pollution”). It seems the definition of partial correlation here is somewhat different with my understanding.

**Reply:** Figure 6 and Figure 7 in the original manuscript mainly aimed at analyzing the dependence of CG lightning on thermodynamic factors and cloud-related factors, so we analyzed the partial correlation between CG lightning and thermodynamic factors (CAPE, RH, and SHEAR) as well as lightning and cloud-related factors (CBH, TCLW, and TCIW), respectively. Based on your comment and Zhao et al. (2019), we recalculated the partial correlation coefficients between six meteorological factors (CAPE, RH, SHEAR, CBH, TCLW, and TCIW) and CG lightning in order to analyze the contribution of individual meteorological factor by eliminating the potential dependence on other meteorological factors. The corresponding discussion was modified, and the following figure was added to the revised manuscript as Figure 7. The details can be seen L436-449 of the revised manuscript.

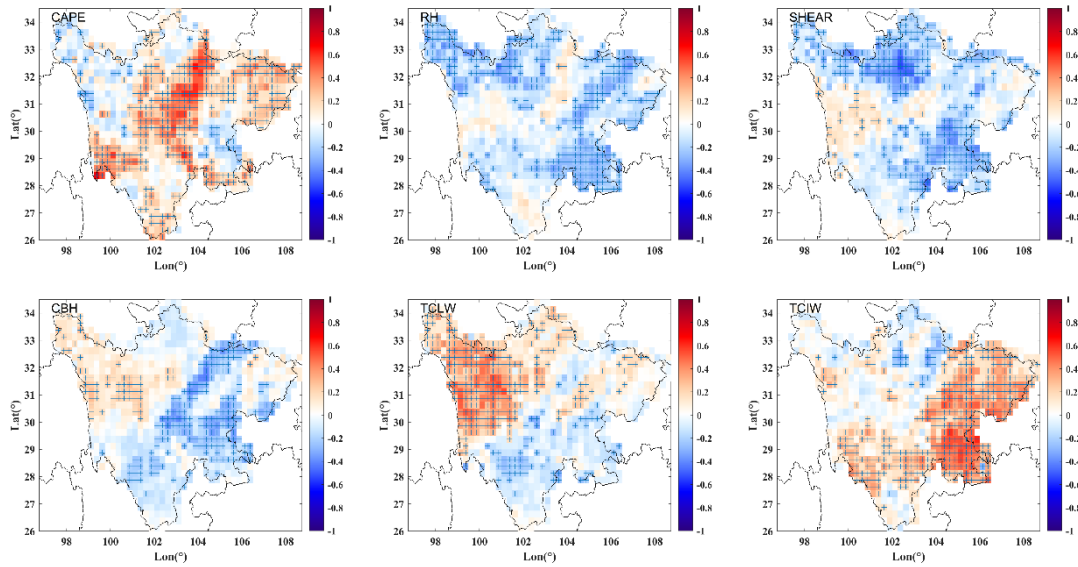


**Figure 7.** Partial correlation coefficients between CG lightning and meteorological factors, i.e., CAPE, RH, SHEAR, CBH, TCLW. Crosses in the figure indicate grid boxes that have passed the 95% significance test.

(6) L318-319, Liu et al. (2019, “Non-Monotonic Aerosol Effect on Precipitation in Convective Clouds over Tropical Oceans”) examined satellite data and also reported a tipping point of precipitation response to aerosol perturbations, which occurs at AOD of 0.3.

**Reply:** We have added this reference in the revised manuscript. The details can be seen L378 of the revised manuscript.

(7) L330, please remove “Compared with the effect of aerosols on lightning activity”, as there is no comparison in this sentence.

**Reply:** It has been removed.

(8) Section 3.5 is confusing. The observed monthly and regional means of lightning density were used to build the multi-variate linear regression model. Then what’s the point to compare the modeled lightning density with the observed one again? Please clarify.

**Reply:** In this study, we discussed the relationship between lightning density and

seven influence factors, including CAPE, RH, SHEAR, CBH, TCLW, TCIW, and AOD. We used Pearson correlation and partial correlation analysis methods to analyze the relative contributions of various influence factors to lightning activity. On this basis, we use multiple linear regression method and stepwise regression method to establish a model, which is used to test whether the seven influencing factors can reproduce the characteristics of lightning activity, and verify the influence factors that contribute more to lightning activity in the plateau and basin region. Previous study (Wang et al., 2018) also used similar methods to discuss the contribution of influence factors to lightning activity in Africa.

(9) L574, please be specific what are the thermodynamic differences.

**Reply:** The thermodynamic difference between the basin region and the plateau region mainly refers to the difference of CAPE. CAPE in the basin region is significantly higher than that in the plateau region, which leads to more vigorous lightning activity in the basin region (Qie et al., 2003). It has been revised accordingly in the revised manuscript. The details can be seen L655-656 of the revised manuscript.

#### **Reference:**

- Karlsson, K. G., Anttila, K., Trentmann, J., Stengel, M., Meirink, J. F., Devasthale, A.: CLARA-A2: the second edition of the CM SAF cloud and radiation data record from 34 years of global AVHRR data. *Atmos. Chem. Phys.*, 17, 5809–5828. <https://doi.org/10.5194/acp-17-5809-2017>, 2017.
- Karlsson, K. G. and Håkansson, N.: Characterization of AVHRR global cloud detection sensitivity. *Atmos. Chem. Phys.*, 11, 633–649. <https://doi.org/10.5194/amt-11-633-2018>, 2018.
- Qie, X., Toumi, R., Zhou, Y. J.: Lightning activity on the central Tibetan Plateau and its response to convective available potential energy, *Chinese Science Bulletin*, 48(3), 296–299, <https://doi.org/10.1007/BF03183302>, 2003.
- Wang, Y., Khalizov, A., Levy, M. and Zhang, R.: New Directions: Light absorbing aerosols and their atmospheric impacts. *Atmos. Environ.*, 81, 713–715,

<https://doi.org/10.1016/j.atmosenv.2013.09.034>, 2013.

Wang, Q., Li, Z., Guo, J., Zhao, C. and Cribb, M.: The climate impact of aerosols on the lightning flash rate: is it detectable from long-term measurements?, *Atmos. Chem. Phys.*, 18(17), 12797–12816, <https://doi.org/10.5194/acp-18-12797-2018>, 2018.

Wei, J., Peng, Y., Mahmood, R., Sun, L. and Guo, J., 2019. Intercomparison in spatial distributions and temporal trends derived from multi-source satellite aerosol products. *Atmos. Chem. Phys.*, 19, 7183–7207, <https://doi.org/10.5194/acp-19-7183-2019>, 2019.

Zhao, B., Wang, Y., Gu, Y., Liou, K.N., Jiang, J.H., Fan, J., Liu, X., Lei, H., Yung, Y.L.: Ice nucleation by aerosols from anthropogenic pollution. *Nat. Geosci.*, 12, 602–607, <https://doi.org/10.1038/s41561-019-0389-4>, 2019.

1 **Distinct aerosol effects on cloud-to-ground lightning in the**  
2 **plateau and basin regions of Sichuan, Southwest China**

3  
4 Pengguo Zhao<sup>1,2,3</sup>, Zhanqing Li<sup>2</sup>, Hui Xiao<sup>4</sup>, Fang Wu<sup>5</sup>, Youtong Zheng<sup>2</sup>,  
5 Maureen C. Cribb<sup>2</sup>, Xiaoai Jin<sup>5</sup>, Yunjun Zhou<sup>1</sup>

6  
7 <sup>1</sup>Plateau Atmosphere and Environment Key Laboratory of Sichuan Province, College  
8 of Atmospheric Science, Chengdu University of Information Technology, Chengdu  
9 610225, China

10 <sup>2</sup>Department of Atmospheric and Oceanic Science, Earth System Science  
11 Interdisciplinary Center, University of Maryland, College Park, MD 20742, USA

12 <sup>3</sup>Key Laboratory for Cloud Physics of China Meteorological Administration, Beijing  
13 100081, China

14 <sup>4</sup>Guangzhou Institute of Tropical and Marine Meteorology, China Meteorological  
15 Administration, Guangzhou 510640, China

16 <sup>5</sup>State Laboratory of Remote Sensing Sciences, College of Global Change and Earth  
17 System Science, Beijing Normal University, Beijing 100875, China

18  
19 Correspondence: Zhanqing Li (zhanqing@umd.edu) and Pengguo Zhao  
20 (zpg@cuit.edu.cn)



28 **Abstract.** The joint effects of aerosol, thermodynamic, and cloud-related factors on  
29 cloud-to-ground lightning in Sichuan were investigated by a comprehensive analysis of  
30 ground measurements made from 2005 to 2017 in combination with reanalysis data.  
31 Data include aerosol optical depth, cloud-to-ground (CG) lightning density, convective  
32 available potential energy (CAPE), mid-level relative humidity, lower- to mid-  
33 tropospheric vertical wind shear, cloud-base height, total column liquid water (TCLW),  
34 and total column ice water (TCIW). Results show that CG lightning density and  
35 aerosols are positively correlated in the plateau region and negatively correlated in the  
36 basin region. Sulfate aerosols are found to be more strongly associated with lightning  
37 than total aerosols, so this study focuses on the role of sulfate aerosols in lightning  
38 activity. In the plateau region, the lower aerosol concentration stimulates lightning  
39 activity through microphysical effects. Increasing the aerosol loading reduces the cloud  
40 droplet size, reducing the cloud droplet collision-coalescence efficiency and inhibiting  
41 the warm-rain process. More small cloud droplets are transported above the freezing  
42 level to participate in the freezing process, forming more ice particles and releasing  
43 more latent heat during the freezing process. Thus, an increase in aerosol loading  
44 increases CAPE, TCLW, and TCIW, stimulating CG lightning in the plateau region. In  
45 the basin region, by contrast, the higher concentration of aerosols inhibits lightning  
46 activity through the radiative effect. An increase in aerosol loading reduces the amount  
47 of solar radiation reaching the ground, thereby lowering CAPE. The intensity of  
48 convection decreases, resulting in less supercooled water transported to the freezing  
49 level and fewer ice particles forming, thus increasing the total liquid water content.  
50 Therefore, an increase in aerosol loading suppresses the intensity of convective activity  
51 and CG lightning in the basin region.

52  
53  
54  
55  
56

57 **1 Introduction**

58

59 Aerosol-cloud-precipitation interactions are complicated, mainly reflected in the  
60 influence of aerosols on cloud microphysical and radiation processes, i.e., aerosol-cloud  
61 interactions (ACI) and aerosol-radiation interactions (ARI) (Rosenfeld et al., 2008;  
62 Huang et al., 2009; Koren et al., 2014; Li et al., 2011, 2017, 2019; Oreopoulos et al.,  
63 2020). The aerosol microphysical effect refers to the role of aerosols as cloud  
64 condensation nuclei (CCN) and ice nuclei (IN), influencing the microphysical  
65 processes of liquid- and ice-phase clouds. The aerosol radiation effect refers to the  
66 absorption and scattering of solar radiation by aerosols, changing the radiation balance  
67 between the atmosphere and the surface. The microphysical and radiative effects of  
68 aerosols combined with dynamic processes influence weather and climate processes  
69 through their links with meteorological conditions.

70 Lightning activity is mainly affected by atmospheric thermodynamic conditions  
71 and is an important indicator of the development of convective systems. The collision  
72 and separation of large and small ice particles mainly cause electrification. Supercooled  
73 water, ice particles, and strong updrafts are the components needed for the occurrence  
74 and development of lightning (MacGorman et al., 2001; Mansell et al., 2005; Williams,  
75 2005; Price, 2013; Q. Wang et al., 2018; Qie and Zhang, 2019).

76 The differences in thermal conditions and aerosol loading between land and ocean  
77 areas lead to a higher lightning frequency over land than over oceans (Williams and  
78 Stanfill, 2002; Williams et al., 2004). Lightning activity over cities with higher aerosol  
79 concentrations are more intense than that over clean suburbs (Westcott, 1995; Pinto et  
80 al., 2004; Kar et al., 2009; Kar and Liou, 2014; Proestakis et al., 2016; Yair, 2018;  
81 Tinmaker et al., 2019). An increase in aerosol concentration leads to the formation of  
82 more small cloud droplets, which have difficulty forming raindrops due to their low  
83 collision-coalescence efficiency, thus inhibiting the warm-rain process. These small  
84 cloud droplets are transported above the freezing level, increasing the supercooled  
85 water content in a thunderstorm and significantly enhancing the ice-phase process. The

86 freezing process releases more latent heat to stimulate convection, allowing more ice  
87 particles to participate in the electrification process of collision and separation, thus  
88 enhancing lightning activity (Khain et al., 2008; Mansell and Ziegler, 2013; P. Zhao et  
89 al., 2015; Shi et al., 2015). A similar enhancement in lightning activity due to aerosols  
90 was also found in oceanic regions, where aerosols and their precursors discharged by  
91 ships significantly enhanced lightning activity over ship lanes (Thornton et al., 2017).  
92 The influence of aerosols on thunderstorms is not linear. When the aerosol optical depth  
93 (AOD) is less than 0.3, aerosols can stimulate lightning activity. However, the intensity  
94 of lightning activity will be inhibited if the concentration of aerosols increases (Altaratz  
95 et al., 2010; Stallins et al., 2013; X. Li et al., 2018; Q. Wang et al., 2018).

96 The effect of aerosols on convective clouds and lightning activity is not only  
97 controlled by environmental factors, but also by aerosol type. Absorbing aerosols in the  
98 boundary layer warm the atmosphere and cool the surface, which leads to the increase  
99 of atmospheric convective inhibition energy and the rise of convection condensation  
100 level (CCL), meanwhile the absorbing aerosols also leads to the increase of convective  
101 available potential energy above CCL. Once the lifting condition overcomes the  
102 convective inhibition energy, strong convective activity will be triggered (Wang et al.,  
103 2013).~~Absorbing aerosols block solar radiation from reaching the surface through~~  
104 ~~radiative effects, which tends to inhibit the development of convection.~~ Hygroscopic  
105 aerosols can stimulate the development of thunderstorms through microphysical effects  
106 under appropriate environmental conditions (Wang et al., 2018). In central China,  
107 aerosol absorption of solar radiation has increased the stability of the lower atmosphere,  
108 reducing thunderstorm activity by 50% from 1961 to 2000 (Yang et al., 2013). In  
109 Nanjing in eastern China, aerosols reduced the amount of solar radiation reaching the  
110 surface and the convective available potential energy (CAPE), inhibiting the intensity  
111 of lightning activity (Tan et al., 2016). In the Sichuan Basin, with its complex  
112 topography, the influence of absorbing aerosols on strong convection is more  
113 complicated. During the day, aerosols absorb solar radiation and increase the stability  
114 of the lower atmosphere, accumulating a large amount of water vapor and energy in the

115 basin. Under the influence of the uplift of the mountain terrain at night, convection is  
116 excited, and stronger convective precipitation is formed in the mountainous area (Fan  
117 et al., 2015). In southeast China where the hygroscopicity of aerosols dominates, an  
118 increase in aerosols in the plain areas significantly stimulates lightning activity (Yuan  
119 et al., 2011; ~~Y.~~ Wang et al., 2011), while the influence of aerosols on thunderstorms in  
120 mountainous areas with slightly higher altitudes is not prominent (Yang and Li, 2014).  
121 Aerosol radiative and microphysical effects have different impacts on thunderstorms at  
122 different stages of their development. In the Pearl River Delta region, the daytime  
123 radiative effect delays lightning activity, while the aerosol microphysical effect at night  
124 further stimulates lightning activity (Guo et al., 2016; Lee et al., 2016).

125 Sichuan province is in southwest China, with the Qinghai-Tibet Plateau and  
126 Hengduan Mountains to the west, the Qinba Mountains to the north, and the Yunnan-  
127 Guizhou Plateau to the south. The western part of Sichuan province is dominated by  
128 plateau and mountainous terrain, with an average elevation of about 2000 to 4000 m,  
129 while the eastern part is dominated by a basin and hilly terrain, with an average  
130 elevation of 300 to 700 m. The eastern part of Sichuan province is a large basin, and the  
131 western part is the easternmost part of the Tibetan Plateau. The thermal and moisture  
132 conditions in the basin facilitate lightning activity (Xia et al., 2015; Yang et al., 2015).  
133 The Sichuan basin is an area with high aerosol loading and with complex terrain not  
134 conducive to pollutant diffusion dispersion (~~X.~~ Zhang et al., 2012; ~~L.~~ Sun et al., 2016;  
135 Wei et al., 2019a, b; Ning et al., 2018a; 2019).

136 There are significant geographical and environmental differences between the  
137 western Sichuan plateau and the eastern Sichuan basin. The thermal conditions of the  
138 western Sichuan Plateau are obviously weaker than those of the Sichuan Basin (Qie et  
139 al., 2003), and the aerosol concentration in the plateau is also significantly lower than  
140 that in the basin (Ning et al., 2018a). Previous studies (Yuan et al., 2011; Wang et al.,  
141 2011; Yang and Li, 2014; Fan et al., 2015) have suggested that aerosol effects on  
142 lightning activity differ significantly due to differences in topography and aerosol. The  
143 purpose of this study is to investigate any similarities and differences in the effects of

144 aerosols on lightning activity in the context of different topography and aerosol  
145 concentrations between the Western Sichuan Plateau and Sichuan Basin.

146 In this study, we investigate the joint effects of aerosol, thermodynamic, and cloud-  
147 related conditions on cloud-to-ground (CG) lightning activity under such special  
148 topographic conditions.

149 ~~We mainly focus on the influence of aerosol, thermodynamic, and microphysical~~  
150 ~~factors on CG lightning density. Previous studies have suggested that aerosols affect~~  
151 ~~the intensity and polarity of lightning (Lyons et al., 1998; Naccarato et al., 2003; Carey~~  
152 ~~et al., 2007; Pawar et al., 2017). Future studies involving observational data analyses~~  
153 ~~and numerical simulations will investigate the mechanism by which aerosols affect the~~  
154 ~~lightning polarity by modulating the charge structure.~~ This paper is organized as follows.  
155 Section 2 describes the data and methodology used in the study. Section 3 presents and  
156 discusses the results, and section 4 summarizes the study.

## 157

## 158 **2 Data and methodology**

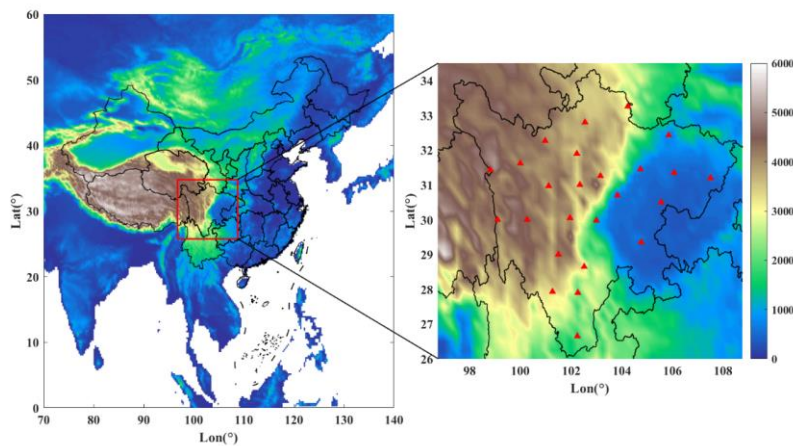
### 159 **2.1 CG lightning**

160 ~~Sichuan province is in southwest China, with the Qinghai Tibet Plateau and~~  
161 ~~Hengduan Mountains to the west, the Qinba Mountains to the north, and the Yunnan-~~  
162 ~~Guizhou Plateau to the south (Fig. 1). The western part of Sichuan province is~~  
163 ~~dominated by plateau and mountainous terrain, with an average elevation of about 2000~~  
164 ~~to 4000 m, while the eastern part is dominated by a basin and hilly terrain, with an~~  
165 ~~average elevation of 300 to 700 m.~~

166 Hourly CG lightning flashes data from 2005 to 2017 were obtained from the  
167 Sichuan Meteorological Bureau. CG lightning flashes are observed by the Sichuan  
168 Lightning Detection Network (SLDN), which belongs to the China Lightning Detection  
169 Network of the China Meteorological Administration (CMA), and consists of 25  
170 detection sensors (Fig. 1). The average detection accuracy of the sensor is ~300 m, the  
171 average detection radius is 300 km, and the detection efficiency is 80–90% (Yang et al.,  
172 2015). The SLDN is based on the ground-based Advanced Time of Arrival and

173 Direction system, which uses improved accuracy from the combined technology  
174 method (Cummins et al., 1998; CMA, 2009).

175 Positive CG lightning flashes with peak currents less than 15 kA are removed to  
176 avoid the contamination of cloud-to-cloud lightning (Cummins and Murphy, 2006). A  
177 flash is identified if the location of the first stroke is within 10 km, and the time interval  
178 between two contiguous strokes is less than 0.5 seconds. If the polarity of the stroke is  
179 different, it is a different flash (Cummins et al., 1998). To match the thermodynamic  
180 and cloud-related parameters, the CG lightning data used in this study were calculated  
181 at a 0.25° horizontal resolution. Many previous studies (e.g., Orville et al., 2011; Ramos  
182 et al., 2011; Yang et al., 2015) have also discussed the basic characteristics of lightning  
183 at a similar resolution.



184  
185 **Figure 1.** Location of Sichuan province with the color-shaded background showing  
186 terrain heights (unit: m). The zoomed image shows the locations of the lightning sensors  
187 (red triangles).

188  
189 **2.2 AOD**

190 The Modern-Era Retrospective analysis for Research and Applications, version 2  
191 (MERRA-2), dataset provided AODs from 2005 to 2017. The quality-controlled  
192 MERRA-2 AOD product (at 550 nm) provides the optical thicknesses of different types  
193 of aerosols, including total aerosol, sulfate, black carbon, organic carbon, and dust, with

194 a spatial resolution of  $0.5^{\circ} \times 0.625^{\circ}$  (Randles et al., 2017; Buchard et al., 2017). To  
195 match CG lightning data, we interpolated AOD data onto the same  $0.25^{\circ}$  spatial  
196 resolution grid. The horizontal distribution and vertical structure of MERRA-2 aerosol  
197 optical properties are in good agreement with satellite and aircraft observations  
198 (Buchard et al., 2017). ~~E.~~ Sun et al. (2018, 2019) employed MODerate resolution  
199 Imaging Spectroradiometer (MODIS) and Aerosol Robotic Network (AERONET)  
200 AOD products to evaluate the MERRA-2 AOD over China. They reported that the  
201 MERRA-2 and MODIS AODs agreed well and that the seasonal correlation coefficients  
202 between the MERRA-2 and AERONET AODs ranged from 0.87 to 0.92. Figure S1  
203 shows the spatial distribution of AOD based on the monthly data of MEERA2 and  
204 Multi-angle Imaging Spectro Radiometer (MISR) data sets from 2005 to 2017. It can  
205 be seen from Fig S1 that the AOD spatial distribution of MISR is very close to that of  
206 MERRA-2, but the AOD value of MISR is smaller than that of MERRA-2. Wei et al.  
207 (2019c) suggest that there is a good consistency between MISR and MODIS AOD  
208 products in southwest China by using multi-satellite data comparison.

### 209 **2.3 Thermodynamic and cloud-related parameters**

210 Thermodynamic and cloud-related factors include CAPE, mid-level relative  
211 humidity (RH), lower- to mid-tropospheric vertical wind shear (SHEAR), cloud-base  
212 height (CBH), total column liquid water (TCLW), and total column ice water (TCIW),  
213 collected from ERA5 reanalysis data with a spatial resolution of  $0.25^{\circ} \times 0.25^{\circ}$  (Dee et  
214 al., 2011).

215 Hoffmann et al. (2019) indicated that the ERA5 reanalysis is more representative  
216 of atmospheric convection, mesoscale cyclones, and mesoscale to synoptic-scale  
217 atmospheric characteristics than the earlier ERA-Interim reanalysis. Freychet et al.  
218 (2020) found that the dry-bulb temperature, wet-bulb temperature, and RH of the ERA5  
219 reanalysis were representative through comparisons with ground observations made in  
220 China. ~~S.~~ Lee et al. (2018) compared the water vapor and liquid water distributions  
221 observed by a microwave radiometer in Seoul, South Korea, with that of the ERA5  
222 reanalysis and found that they agreed well. Shou et al. (2019) confirmed that ERA5

223 data captured the cloud-top features based on multi-satellite observations made over the  
224 Tibetan Plateau. Zhang et al. (2019) pointed out that the ERA5 precipitable water vapor  
225 field agreed well with radiosonde and Global Navigation Satellite System observations.  
226 Lei et al. (2020) examined the representation of ERA5 cloud-cover characteristics over  
227 China through comparisons with satellite observations, reporting that (1) ERA5  
228 overestimated the cloud cover by ~10%, and (2) the long-term trend in ERA5 cloud  
229 cover was consistent with satellite observations. These studies suggest that ERA5  
230 cloud-related data from China have sound quality. We compared LWPs and IWPs of  
231 CLARA-A2 and ERA5 data sets. The monthly CLARA-A2 record with a spatial  
232 resolution of 0.25°×0.25° provides cloud properties, surface albedo, and surface  
233 radiation parameters derived from the Advanced Very High-Resolution Radiometer  
234 (AVHRR) sensor (Karlsson et al., 2017; Karlsson and Håkansson, 2018). And overall,  
235 the cloud products of the two data sets were similar (Figure S2). For the continuity of  
236 data, LWP and IWP in ERA5 were selected in this study.

237 CAPE is the most important factor controlling lightning, and climate projections  
238 suggest that an increase in CAPE caused by global warming could increase global  
239 lightning by 50% in the twenty-first century (Romps et al., 2014). The proxy composed  
240 of precipitation rate and CAPE has a good correlation with observed lightning density  
241 over the United States (Romps et al., 2018; Tippett and Koshak, 2018; Tippett et al.,  
242 2019). CAPE is the factor with the highest relative contribution in various lightning  
243 parameterization schemes (Bang and Zipser, 2016; Stolz et al., 2015, 2017).

244 Due to the large elevation fluctuation in Sichuan, pressure-level data are not  
245 applicable to the analysis of the atmospheric vertical structure. So, pressure levels were  
246 changed to geometric altitudes above ground level (AGL), using the barometric formula  
247 (Minzner, 1977)

$$248 \quad Z_2 = Z_1 + 18410 \left( 1 + \frac{t_a}{273.15} \right) \log \frac{P_1}{P_2}, \quad (1)$$

249 where  $Z_2$  and  $Z_1$  are the elevations of the two isobaric levels (in m),  $P_2$  and  $P_1$  are the  
250 pressures of the two isobaric levels (in hPa),  $P_1$  is 1000 hPa,  $Z_1$  is 0 m, and  $t_a$  is the  
251 average temperature of the two isobaric levels (in °C). The elevation minus topographic



252 height is the altitude AGL,

253 
$$H = Z_2 - H_t, \quad (2)$$

254 where  $H$  is the geometric altitude AGL, and  $H_t$  is the topographic height.

255 The mid-level RH and the lower- to mid-tropospheric SHEAR are important  
256 humidity and dynamic parameters, directly affecting the formation, development,  
257 propagation, and intensity of thunderstorms (Davies-Jones, 2002; Thompson et al.,  
258 2007; Wall et al., 2014; Bang and Zipser, 2016). In this study, RH is the average RH in  
259 the 3–5-km layer, and SHEAR is the vertical wind shear in the 0–5-km layer:

260 
$$SHEAR = \sqrt{(u_2 - u_1)^2 + (v_2 - v_1)^2}, \quad (3)$$

261 where  $u_2$ ,  $u_1$ ,  $v_2$ , and  $v_1$  are zonal and meridional wind speeds at 5 km and 3 km,  
262 respectively.

263 CBH, TCLW, and TCIW were selected to represent cloud-related parameters  
264 affecting the development of lightning activity. CBH, negatively correlated with the  
265 warm-cloud thickness, controls the convective structure and the polarity and intensity  
266 of CG lightning by affecting the liquid water and ice water contents (Williams et al.,  
267 2005; Carey and Buffalo, 2007; Stolz et al., 2017). Liquid water and ice water,  
268 especially in the non-inductive electrification zone, directly control the processes of  
269 charge generation and separation that determines the intensity of lightning of a  
270 thunderstorm (Yair et al., 2010; Wong et al., 2013; Dafis et al., 2018).

271 In this study, we use Pearson correlation and partial correlation to discuss the  
272 relationship between two elements at each grid point. Data from 156 months during the  
273 period 2005–2017 were used, and monthly averages were calculated. Data at each grid  
274 point were processed using a three-point moving average. [Table 1 shows the acronyms  
275 of variables in this study.](#)

276 **Table 1. Acronyms of variables in this study**

| <u>Acronym</u> | <u>Variable</u>                              |
|----------------|--|
| <u>AOD</u>     | <u>Aerosol optical depth</u>                 |
| <u>CAPE</u>    | <u>Convective available potential energy</u> |
| <u>CBH</u>     | <u>Cloud base height</u>                     |

设置了格式: 字体: 加粗

带格式的: 居中

带格式表格

|              |   |
|--------------|---|
| <u>RH</u>    | <u>Mid-level relative humidity</u>                    |
| <u>SHEAR</u> | <u>Lower- to mid-tropospheric vertical wind shear</u> |
| <u>TCLW</u>  | <u>Total column liquid water</u>                      |
| <u>TCIW</u>  | <u>Total column ice water</u>                         |

---

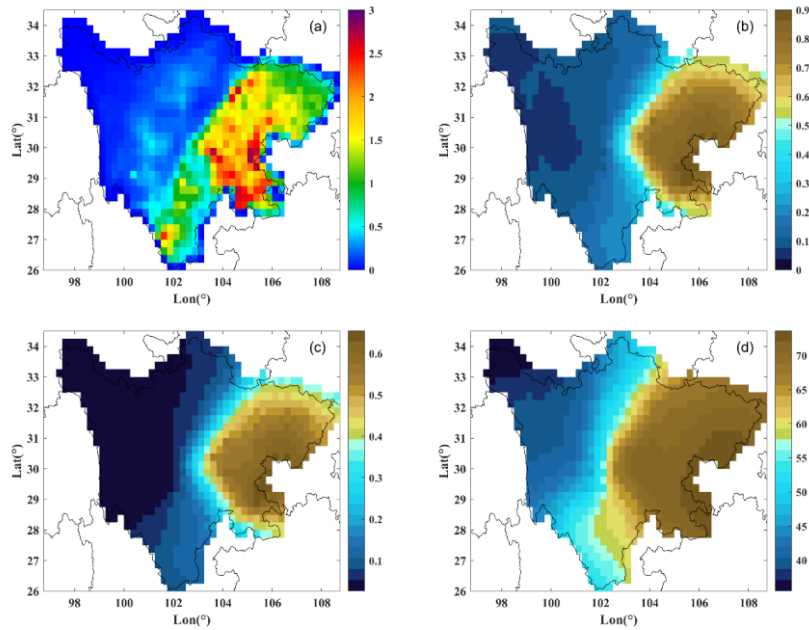
277

### 278 **3 Results and discussion**

#### 279 **3.1 Distributions of CG lightning and AOD**

280 Due to the complex terrain in Sichuan, the CG lightning density and AOD differ  
 281 greatly across the province. The CG lightning density is highest over the basin region  
 282 in eastern Sichuan, with an annual average density of 1–3 flashes km<sup>-2</sup> yr<sup>-1</sup> (Fig. 2a).  
 283 The lightning density in western Sichuan is much lower than that in the basin region.  
 284 Yang et al. (2015) showed that the Sichuan basin is one of the most CG-lightning-active  
 285 regions in China, besides the Yangtze River Delta and the Pearl River Delta. The  
 286 dramatic difference in lightning density between the basin and the plateau stems  
 287 primarily from differences in humidity and thermal conditions. Another factor is the  
 288 generation of strong convective systems caused by the eastward migration of the  
 289 southwest vortex formed over the Tibetan Plateau to the basin area (Yu et al., 2007;  
 290 Zhang et al., 2014). The total AOD over the basin region is significantly higher than  
 291 that over the plateau region. The mean AOD over the basin is about 0.6–0.9, while that  
 292 over the plateau is about 0.15 (Fig. 2b). The aerosols in Sichuan are mainly composed  
 293 of sulfate aerosols, accounting for about 60–80% of the total AOD over the basin and  
 294 40–55% of the total AOD over the plateau (Fig. 2d). Aerosol concentrations over the  
 295 basin are higher than those over the plateau area, mainly because of the greater amount  
 296 of anthropogenic air pollutants emitted in the basin (Zhang et al., 2012). Also playing  
 297 important roles are the mountains around the basin and the low-pressure system at 700  
 298 hPa over the basin, resulting in a strong inversion above the planetary boundary layer  
 299 (Ning et al., 2018<sup>b</sup>).

带格式的: 缩进: 首行缩进: 0 字符



300 **Figure 2.** Distribution of (a) CG lightning density (unit: flashes km<sup>-2</sup> yr<sup>-1</sup>), (b) total  
 301 AOD, (c) sulfate AOD, and (d) percentage of sulfate AOD in total AOD (unit: %) over  
 302 Sichuan.

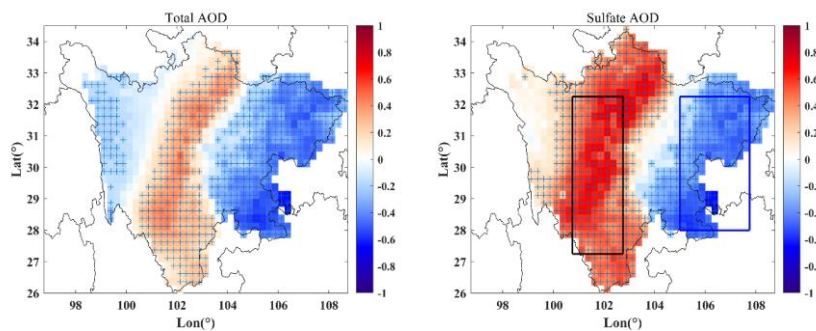
303

### 304 3.2 Correlation between AOD and CG lightning

305 While the spatial patterns of lightning intensity (Fig. 2a) and AOD (Fig. 2b) bear  
 306 some resemblance, one cannot draw a straight conclusion that the latter is the cause of  
 307 the former because they are both **affected/influenced** by the topography. However, the  
 308 influences of aerosols on lightning have been well established in previous studies by  
 309 affecting the local meteorological environment through aerosol radiative and  
 310 microphysical effects (Yang et al., 2013; Q. Wang et al., 2018; Z. Li et al., 2019). To  
 311 circumvent the topographic influence, Fig. 3 shows the Pearson correlation coefficients  
 312 of total AOD/sulfate AOD and CG lightning density in individual grid boxes in Sichuan.  
 313 It is interesting to note that the correlation between aerosol loading and lightning is  
 314 opposite in the plateau region and the basin region, i.e., a positive correlation in the  
 315 plateau region and a negative correlation in the basin region. This suggests that aerosols  
 316 stimulate lightning in the plateau region, but suppress lightning in the basin region.

317 Such a distinct difference may be related to differences in aerosol loading and local  
 318 environmental factors (Rosenfeld et al., 2007; Fan et al., 2009; Carrió and Cotton, 2014).  
 319 The maximum value of the positive correlation coefficient was about 0.5, occurring in  
 320 the plateau region of central Sichuan. The maximum values of the negative correlation  
 321 coefficients occurred in the basin region of eastern Sichuan. The absolute values of the  
 322 negative correlation coefficients are larger than those of the positive correlation  
 323 coefficients. The distribution of the correlation coefficients between lightning and  
 324 sulfate AOD is similar to that of total AOD, but there are more and larger positive  
 325 correlation coefficients than negative ones. Since sulfate AOD accounts for about 60-  
 326 80% of the total AOD over the basin region and 40-55% of the total AOD over the  
 327 plateau region ~~accounts for more than 80% of the total AOD in Sichuan~~, this study  
 328 mainly discusses the relationship between sulfate AOD and lightning activity.

329 ~~Note that a statistical relationship between two variables does not necessarily~~  
 330 ~~imply a true causality between the two for which much further insights are needed. The~~  
 331 ~~spatial contrast exhibited in the correlation maps, however, conveys valuable~~  
 332 ~~information about the causality because the influences of large scale meteorology may~~  
 333 ~~have little to do with the spatial pattern.~~ The plateau and basin regions in this study are  
 334 outlined in Fig. 3 (right panel) to discuss the effects of sulfate aerosols on lightning  
 335 activity in the two regions separately.



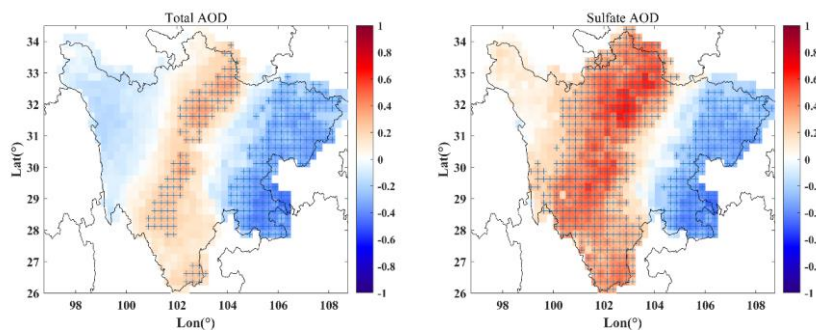
336 **Figure 3.** Pearson correlation coefficients between total AOD and CG lightning (left  
 337 panel) and sulfate AOD and CG lightning (right panel) based on monthly data from  
 338 2005 to 2017. The correlation coefficient of each grid box is calculated from 156  
 339 monthly average datasets, and monthly average data are processed using a three-point  
 340 moving average. Crosses in the figure indicate grid boxes that have passed the 95%

341 significance test. The plateau region and the basin region are outlined by black and blue  
342 rectangles, respectively, in the right panel.

343  
344 To further verify the stimulation and inhibition of aerosols on lightning activity  
345 and eliminate the interference of seasonality on the effects of aerosols on lightning,  
346 Pearson correlation coefficients between anomalies of total AOD and CG lightning and  
347 anomalies of sulfate AOD and CG lightning were implemented. As can be seen from  
348 the comparison between Fig. 3 and Fig. 4, the correlation coefficients between the  
349 anomalies of AOD and lightning are significantly lower than those between AOD and  
350 lightning. While in an overall view, there is still a positive correlation between aerosols  
351 and lightning in the plateau region, and a negative correlation between aerosols and  
352 lightning in the basin region, especially for sulfate aerosols. This further verifies that  
353 aerosols have the potential to stimulate lightning activity in the plateau region and  
354 inhibit lightning activity in the basin region. The specific physical relationship will be  
355 further discussed below.

356 Note that a statistical relationship between two variables does not necessarily  
357 imply a true causality between the two for which much further insights are needed. The  
358 spatial contrast exhibited in the correlation maps, however, conveys valuable  
359 information about the causality because the influences of large-scale meteorology may  
360 have little to do with the spatial pattern.

带格式的: 缩进: 首行缩进: 2 字符, 制表位: 3.33 字符, 左对齐

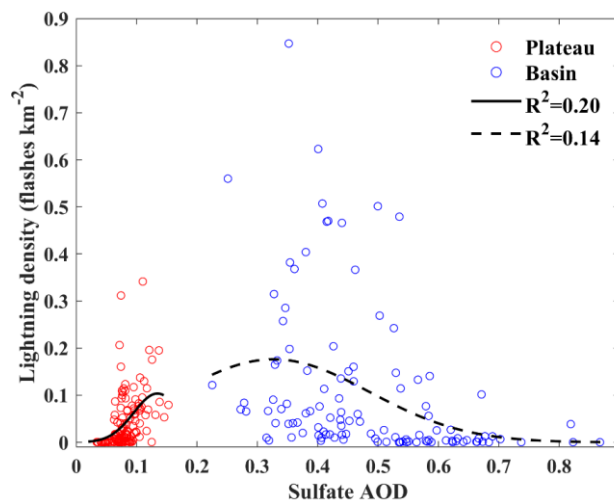


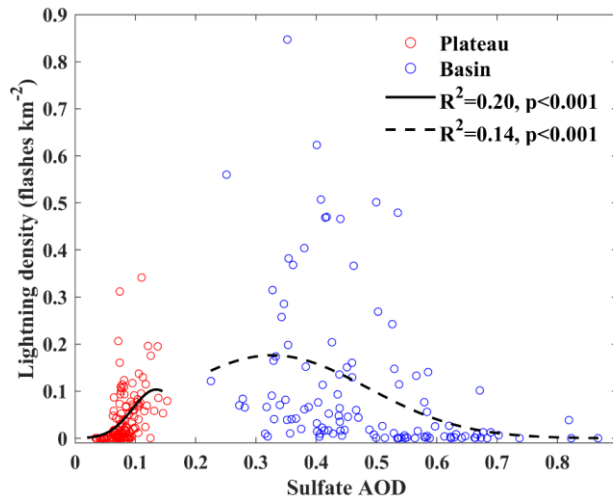
361 **Figure 4.** Pearson correlation coefficients between anomalies of total AOD and CG  
362 lightning (left panel) and anomalies of sulfate AOD and CG lightning (right panel)  
363 based on monthly data from 2005 to 2017. Crosses in the figure indicate grid boxes that  
364 have passed the 90% significance test.

365

366 To further analyze the relationship between aerosols and lightning over Sichuan,  
367 Fig. 45 shows the CG lightning density as a function of sulfate AOD over the plateau  
368 and basin regions. Due to differences in emissions, the aerosol loading over the plateau  
369 region is much lighter than that over the basin region. The regional average sulfate AOD  
370 over the plateau region ranges from 0.03 to 0.15, and that over the basin region ranges  
371 from 0.22 to 0.87. The difference in CG lightning density is mainly related to the  
372 different meteorological conditions of the plateau and the basin. The monthly regional  
373 average CG lightning density over the plateau is  $0.1 \times 10^{-3}$  to  $0.35$  flashes  $\text{km}^{-2}$ , while  
374 that over the basin is  $0.1 \times 10^{-3}$  to  $0.85$  flashes  $\text{km}^{-2}$ . In the plateau region, the lightning  
375 density increases exponentially with increasing AOD, while in the basin region, the  
376 lightning density decreases exponentially with increasing AOD. This difference may be  
377 due to the different microphysical and radiative effects of different aerosol loadings.  
378 Previous studies (Koren et al., 2008, 2012; Altaratz et al., 2010, 2017; [Liu et al., 2019](#))  
379 have noted a turning point of  $\text{AOD} = 0.3$  with regard to the influence of AOD on clouds.  
380 For lower AOD, aerosols can stimulate lightning activity through microphysical effects.  
381 For higher AOD, aerosols reduce the solar radiation reaching the surface through the  
382 radiative effect, thus inhibiting lightning activity.

383





384

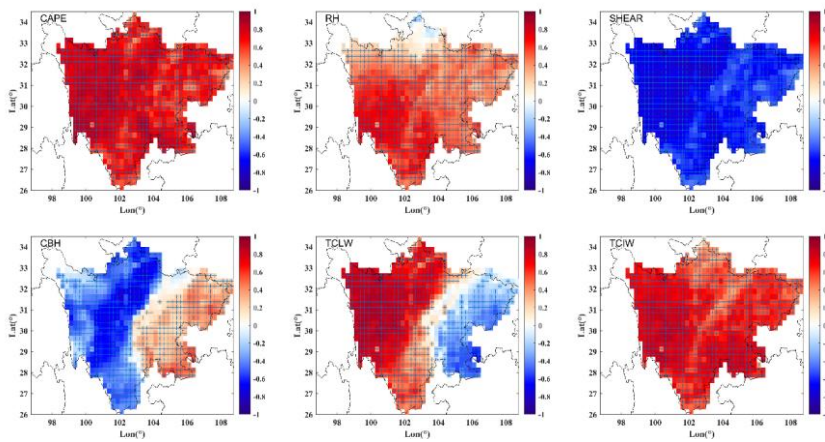
385 **Figure 45.** CG lightning density as a function of sulfate AOD over the basin (blue  
 386 circles) and plateau (red circles) regions. Exponential-fit curves are shown, and  
 387 coefficients of determination ( $R^2$ ) and p values are given.

388

389 **3.3 Correlation between thermodynamic and cloud-related factors and CG**  
 390 **lightning**

391 ~~Compared with the effect of aerosols on lightning activity, thermodynamic~~  
 392 ~~Thermodynamic~~ and cloud-related parameters are the decisive factors determining the  
 393 occurrence and development of lightning activity (Williams, 2005; Williams et al., 2005;  
 394 Saunders, 2008; Stolz et al., 2017). Figure 56 shows correlation coefficients between  
 395 CAPE, RH, SHEAR, CBH, TCLW, and TCIW, and CG lightning density over Sichuan.  
 396 The thermodynamic parameters CAPE and RH, especially CAPE, have significant  
 397 excitation effects on lightning activity, while SHEAR shows a significant negative  
 398 correlation with lightning. There is a positive correlation between TCIW and lightning  
 399 density over Sichuan because the development of lightning mainly depends on the non-  
 400 inductive electrification of the collision and separation of large and small ice particles.  
 401 The more ice particles, the stronger the lightning activity will be. The correlation  
 402 between CBH and lightning is opposite to that between TCLW and lightning in the  
 403 plateau and basin regions. Over the plateau area, low cloud bases and high liquid water

404 contents are favorable for lightning activity, while over the basin, the opposite is seen.  
 405 A higher CBH means that the warm-cloud depth is thinner, so the liquid water content  
 406 will be less. In the plateau region, because of the compression effect of the plateau  
 407 topography on clouds, the warm-cloud depth is much thinner than that in the basin  
 408 region. Increasing a fixed amount of liquid water is conducive to transporting  
 409 supercooled water to the upper layer and promoting the development of the ice-phase  
 410 process. The more vigorous the ice-phase process is, the more intense the lightning  
 411 activity will be. Over the basin, where warm clouds are thicker, an increase in liquid  
 412 water will more likely promote the development of the warm-rain process rather than  
 413 the ice-phase process. Fig. S3 shows the correlation coefficients between the anomalies  
 414 of CAPE, RH, SHEAR, CBH, TCLW, and TCIW and CG lightning. Compared with  
 415 Figure 6, the correlation coefficients are obviously smaller, especially in the basin  
 416 region. The significances of the correlation between CG lightning and environmental  
 417 factors are weakened, especially SHERA, CBH, and TCLW in the basin region.



418 **Figure 56.** Pearson correlation coefficients between CAPE, RH, SHEAR, CBH, TCLW,  
 419 and TCIW and CG lightning. Crosses in the figure indicate grid boxes that have passed  
 420 the 95% significance test.

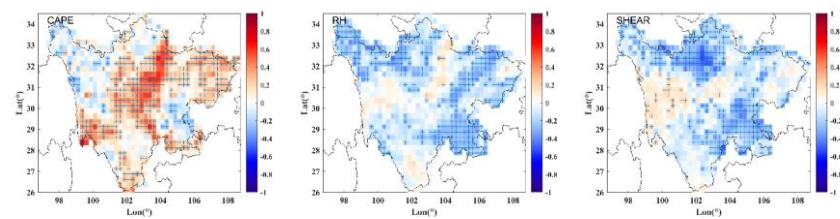
421

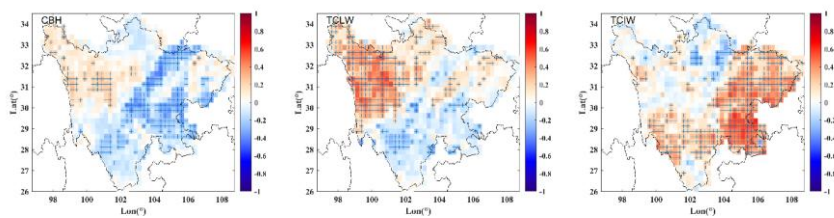
422 The partial correlation analysis was used in many previous studies (Wang et al.,  
 423 2018; Zhao et al., 2019) to discuss the dependence between two variables where the  
 424 influence from other possible variables. To avoid interactions between the factors

带格式的: 缩进: 首行缩进: 2 字符



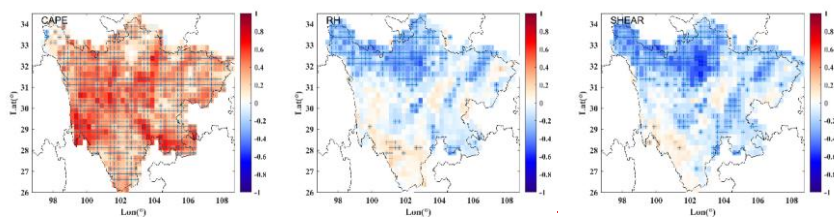
425 involved and to discuss the relationships between different factors and lightning activity  
 426 more independently, Figs. ~~6~~ and ~~7~~, respectively, shows the partial correlation  
 427 coefficients between thermodynamic and cloud-related parameters and CG lightning  
 428 density. In terms of the thermodynamic parameters, the partial correlation coefficients  
 429 show that the dependence of lightning on RH and SHEAR is not significant. The partial  
 430 correlation coefficient of some regions in Sichuan is 0. Compared with RH, the absolute  
 431 value of the negative partial correlation coefficient of SHEAR is larger and more widely  
 432 distributed, indicating that SHEAR has a more significant impact (inhibition) on  
 433 lightning activity than does RH. CAPE is positively correlated with lightning in Sichuan,  
 434 and the partial correlation coefficient of many grid points is greater than 0.42, indicating  
 435 that CAPE is a crucial factor controlling lightning, as reported by others (Carey and  
 436 Buffalo, 2007; Fuchs et al., 2015; Bang and Zipser, 2016; Stolz et al., 2017). Among  
 437 the cloud-related parameters, the partial correlation coefficients between CBH and  
 438 TCLW and lightning are lower, indicating that CBH and TCLW have less significant  
 439 influences on lightning density. The existence of supercooled water is one of the  
 440 essential conditions for the electrification of thunderstorms. The supercooled liquid  
 441 water content in different temperature ranges can affect the polarity of the charge  
 442 carried by ice particles but cannot directly affect the intensity of the electrical activity  
 443 of thunderstorms (Saunders et al., 1991; Saunders, 2008). The positive partial  
 444 correlation coefficient between TCLW and lightning is relatively higher, especially in  
 445 the basin area, indicating that ice particles, as the carrier of charge, can directly  
 446 determine the occurrence and development process of lightning activity.





447 **Figure 7.** Partial correlation coefficients between CG lightning and thermodynamic and  
 448 cloud-related factors, i.e., CAPE, RH, SHEAR, CBH, TCLW. Crosses in the figure  
 449 indicate grid boxes that have passed the 95% significance test.

带格式的: 缩进: 首行缩进: 0 字符, 行距: 单倍行距

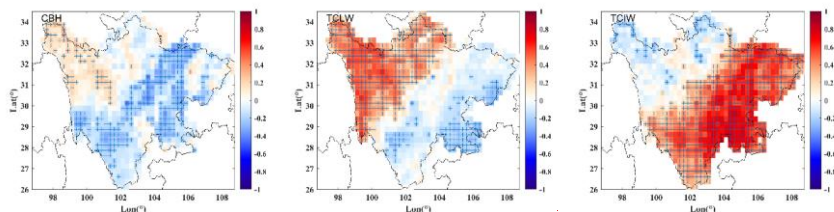


450 **Figure 6.** Partial correlation coefficients between CG lightning and thermodynamic  
 451 factors, i.e., CAPE, RH, and SHEAR. Crosses in the figure indicate grid boxes that have  
 452 passed the 95% significance test.

453

454 Among the cloud-related parameters, the partial correlation coefficients between CBH  
 455 and TCLW and lightning are lower, indicating that CBH and TCLW have less  
 456 significant influences on lightning density (Fig. 7). The existence of supercooled water  
 457 is one of the essential conditions for the electrification of thunderstorms. The  
 458 supercooled liquid water content in different temperature ranges can affect the polarity  
 459 of the charge carried by ice particles but cannot directly affect the intensity of the  
 460 electrical activity of thunderstorms (Saunders et al., 1991; Saunders, 2008). The  
 461 positive partial correlation coefficient between TCLW and lightning is relatively higher,  
 462 especially in the basin area, indicating that ice particles, as the carrier of charge, can  
 463 directly determine the occurrence and development process of lightning activity.

带格式的: 缩进: 首行缩进: 0 字符

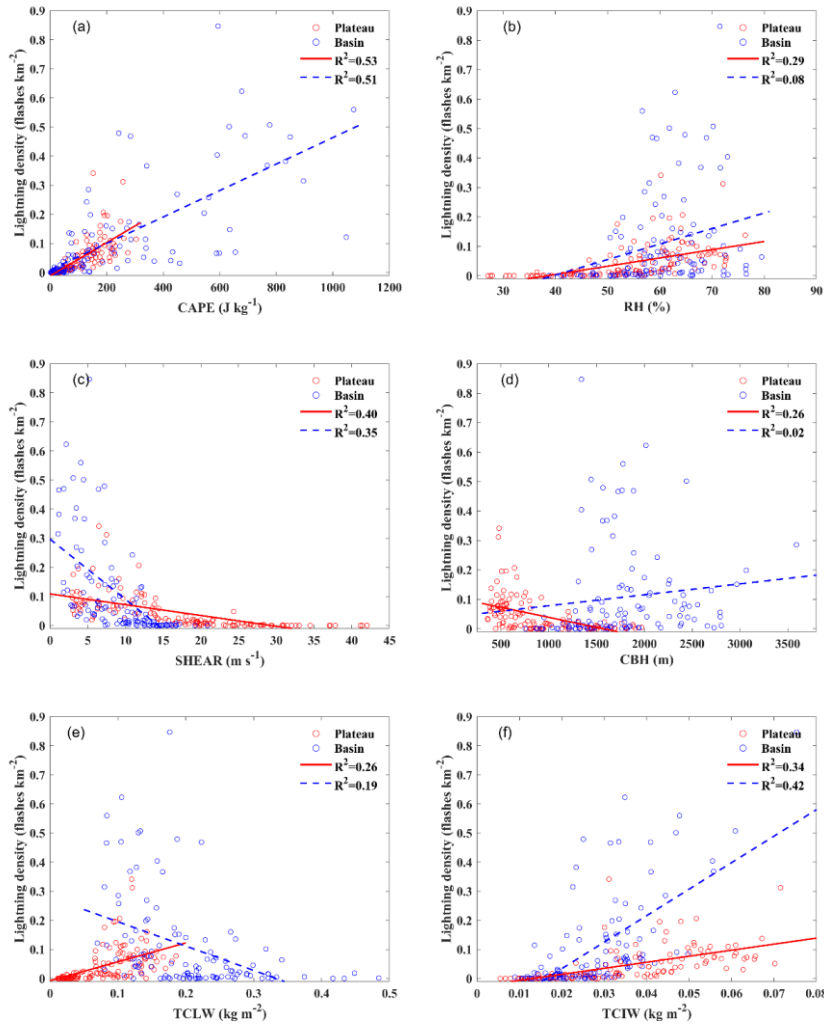


464 ~~Figure 7. Partial correlation coefficients between CG lightning and cloud-related~~  
465 ~~factors, i.e., CBH, TCLW, and TCIW. Crosses in the figure indicate grid boxes that have~~  
466 ~~passed the 95% significance test.~~

467  
468 To demonstrate the differences in thermodynamic and cloud-related factors  
469 between the plateau and basin regions, Fig. 88 shows CG lightning density as a function  
470 of the thermodynamic and cloud-related parameters in the plateau and basin regions,  
471 based on monthly regionally averaged data. There is a significant positive correlation  
472 between CAPE and CG lightning density in both the plateau and basin regions, with a  
473 coefficient of determination ( $R^2$ ) of 0.53 and 0.51, respectively. CAPE over the plateau  
474 region is much smaller than that over the basin region. The maximum CAPE over the  
475 plateau area is  $\sim 300 \text{ J kg}^{-1}$ , while the maximum CAPE over the basin area is ~~over-greater~~  
476  $1000 \text{ J kg}^{-1}$ . This is the main reason why the CG lightning density over the basin region  
477 is larger than that over the plateau region. RH and CG lightning density were positively  
478 correlated in both plateau and basin regions, but not significantly in the basin region  
479 ( $R^2 = 0.08$ ). Due to the high altitude of the plateau and strong wind speeds there,  
480 SHEAR in the plateau region (maximum value of  $40 \text{ m s}^{-1}$ ) is significantly larger than  
481 that in the basin region (maximum value of  $15 \text{ m s}^{-1}$ ). The greater mid-level wind shear  
482 over the plateau region suppresses the intensity of lightning activity.

483 Due to the compression of clouds by the plateau topography, the mean CBH over  
484 the plateau region is relatively low, about 500–2000 m, while the mean CBH over the  
485 basin region is about 1000–3500 m. The correlation between CBH and lightning density  
486 is negative in the plateau. In the basin, however, there is barely any correlation ( $R^2 =$   
487  $0.02$ ). The much lower temperature over the plateau directly results in a lower liquid  
488 water content there. The maximum value of TCLW is  $\sim 0.2 \text{ kg m}^{-2}$ , while that in the  
489 basin region is  $\sim 0.5 \text{ kg m}^{-2}$ . Correlations in the plateau region are more significant than  
490 in the basin region, with an  $R^2$  of 0.26 and 0.19, respectively. The TCIWs over the  
491 plateau and basin areas are similar in magnitude. The positive correlation between  
492 TCIW and lightning density is also significant, with an  $R^2$  of 0.34 and 0.42, respectively,  
493 in the basin and plateau regions. Except for the correlation between CBH and lightning

494 in the basin region, the linear correlations between the other factors and lightning  
 495 passed the 95% significance test.

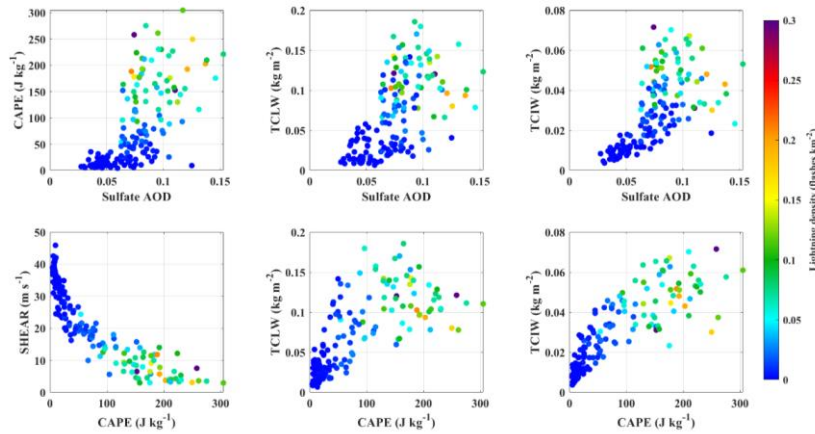


496 **Figure 88.** Lightning density as a function of thermodynamic and cloud-related factors  
 497 in the basin (blue circles) and plateau (red circles) regions: (a) CAPE, (b) RH, (c)  
 498 SHEAR, (d) CBH, (e) TCLW, and (f) TCIW. Linear-fit lines are shown, and coefficients  
 499 of determination ( $R^2$ ) are given.

500

501 **3.4 Joint effects of thermodynamic and cloud-related factors and aerosols on CG**  
 502 **lightning**

503 Based on the partial correlation and linear fitting analyses, CAPE, SHEAR, TCLW,  
504 and TCIW are the main thermodynamic and cloud-related factors controlling CG  
505 lightning over the Sichuan region. To analyze the joint effects of thermodynamic factors,  
506 Figs. [99](#) and [1010](#) show scatter plots between sulfate AOD, CAPE, SHEAR, TCLW,  
507 and TCIW, and CG lightning in the plateau and basin regions. In the plateau region (Fig.  
508 [99](#)), increases in CAPE, TCLW, and TCIW enhance lightning activity. As discussed  
509 before (Fig. [87](#)), strong convective activity and more liquid water and ice water indicate  
510 that strong updrafts transport a greater amount of liquid-phase and ice-phase particles  
511 to the electrification area to participate in the electrification process, generating stronger  
512 lightning activity. Aerosol excitation of lightning may be achieved by increasing CAPE,  
513 TCLW, and TCIW. In the case of low aerosol loading, through ACI, an increase in  
514 aerosols will reduce the size of cloud droplets and increase the concentration of cloud  
515 droplets (Khain et al., 2008; Qian et al., 2009). Smaller cloud droplets reduce the  
516 collision-coalescence efficiency and inhibit the warm-rain process. Small cloud  
517 droplets that do not fall are transported above the freezing layer to participate in the  
518 freezing process and release more latent heat. This is consistent with previous studies  
519 (Mansell et al., 2013; P. Zhao et al., 2015; Altaratz et al., 2017; Fan et al., 2018; C. Zhao  
520 et al., 2018) and explains the potential cause of the increase in aerosols, leading to an  
521 increase in liquid water and ice water in thunderstorms, promoting convective activities.  
522 From the joint influence of CAPE, SHEAR, TCLW, and TCIW on lightning activity  
523 (bottom panels of Fig. [99](#)), an increase in CAPE inhibits the vertical wind shear in the  
524 lower to middle troposphere ([Li et al., 2013](#); [Sherburn et al., 2016](#)), which is conducive  
525 to the development of lightning activity. Increasing CAPE also suggests that strong  
526 updrafts promote the development of convection, resulting in the formation of more  
527 liquid water and ice water in the cloud.

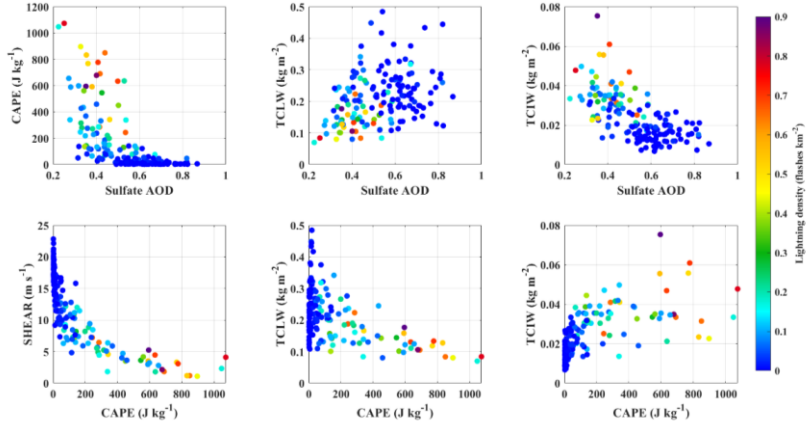


528  
 529 **Figure 99.** Joint effects of sulfate AOD, CAPE, SHEAR, TCLW, and TCIW on CG  
 530 lightning density over the plateau region. The color of the dots represents the CG  
 531 lightning density.

532

533 The aerosol loading over the basin region is much higher than that over the plateau  
 534 region, with sulfate AODs ranging from 0.2 to 0.9 (Fig. 190). Excessive aerosol loading  
 535 inhibits convective development through ARI. Aerosols reduce the solar radiation  
 536 reaching the surface through absorption and scattering, reducing the convective energy  
 537 of the surface and the lower atmosphere (Zhao et al., 2006; Jiang et al., 2018). Thus,  
 538 weak updrafts cannot transport liquid water above the freezing level. This may be why  
 539 the increase in aerosols leads to an increase in liquid water content and a decrease in  
 540 ice water content. Aerosols reduce the intensity of lightning activity by inhibiting the  
 541 development of convection and the formation of ice particles. This has also been  
 542 observed in other regions (Yang et al., 2013; Tan et al., 2016). CAPE is higher over the  
 543 basin region than over the plateau region (bottom panels of Fig. 140). An increase in  
 544 CAPE leads to a decrease in SHEAR and an increase in ice water content, promoting  
 545 the development of lightning, similar to the plateau region. Fan et al. (2009) found that  
 546 under large vertical wind shear conditions, an increase in aerosols inhibits the  
 547 development of convection. However, when CAPE exceeded  $300 \text{ J kg}^{-1}$ , an increase in  
 548 CAPE lead to a decrease in liquid water content. Convective clouds over the basin are

549 thicker than those over the plateau, and the high CAPE makes convection develop more  
 550 vigorously. In this way, liquid water is transported above the freezing level to participate  
 551 in the ice-phase process, forming more ice particles.



552  
 553 **Figure 100.** Same as in Fig. 99, but for the basin region.

554  
 555 According to the above, we hypothesize that the microphysical effect of aerosols  
 556 is responsible for stimulating lightning activity over the plateau region and that the  
 557 radiative effect of aerosols is responsible for suppressing lightning activity over the  
 558 basin region. The radiative effect of aerosols impacts lightning by affecting CAPE,  
 559 while the microphysical effect of aerosols impacts lightning by affecting the liquid  
 560 water and ice water contents. To further verify the radiative effect of aerosols in the  
 561 basin and the microphysical effect of aerosols in the plateau, two lightning sensitivity  
 562 parameters are employed:

$$563 \quad RL_r = FC/CAPE, \quad (4)$$

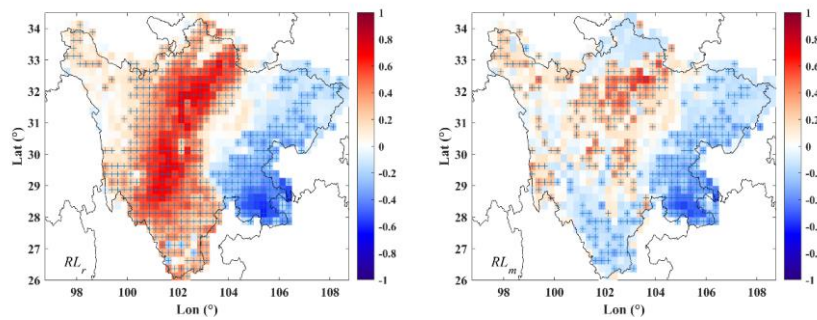
564 where  $RL_r$  is a relative measure of lightning sensitivity to the effect of CAPE, associated  
 565 with the aerosol radiative effect, and  $FC$  is the CG lightning flash count. Tinmaker et  
 566 al. (2019) evaluated the impact of CAPE on lightning over land and oceanic regions by  
 567 using  $FC/CAPE$ :

$$568 \quad RL_m = FC/(CAPE \times TCLW \times TCIW), \quad (5)$$

569 where  $RL_m$  is a relative lightning parameter accounting for the effect of TCLW and

570 TCIW on lightning, associated with the aerosol microphysical effect. Since CAPE is an  
571 essential factor for generating lightning, it is also considered in this formulation.

572 Figure 141 shows the Pearson correlation coefficients between  $RL_r$ ,  $RL_m$ , and  
573 sulfate AOD over Sichuan. Compared with the correlation between sulfate AOD and  
574 CG lightning (right panel of Fig. 3), the negative correlation between sulfate AOD and  
575  $RL_r$  decreased significantly in the basin area, especially in the northern part of the basin,  
576 while the positive correlation between AOD and  $RL_r$  did not change significantly in the  
577 plateau region. This suggests that the inhibitory effect of aerosols on lightning in the  
578 basin region is dependent on the effect on CAPE, but not in the plateau region, which  
579 also reflects the significant radiative effect of aerosols in the basin region. By  
580 comparing the correlation between sulfate AOD and  $RL_m$  (right panel of Fig. 141) and  
581 the correlation between sulfate AOD and CG lightning (right panel of Fig. 3), the  
582 positive correlation coefficients between sulfate AOD and  $RL_m$  in the plateau region  
583 decreased significantly, indicating that aerosols in the plateau region have a significant  
584 microphysical effect, stimulating the development of lightning activity by influencing  
585 liquid- and ice-phase particles in thunderstorms.



586 **Figure 141.** Same as in Fig. 3, but for  $RL_r$  (left panel) and  $RL_m$  (right panel).  
587

### 588 3.5 Multiple linear regression of CG lightning

589 Because the physical processes involved in the development of lightning are  
590 complex, many previous studies (e.g., Allen and Pickering, 2002; Tippet and Koshak,  
591 2018) have parameterized lightning in weather and climate models by statistical



592 regression methods instead of describing the specific physical processes of lightning in  
 593 the model. Stolz et al. (2017) developed a global lightning parameterization scheme  
 594 based on multiple linear regression, combining aerosol and thermodynamic parameters,  
 595 which explained 69–81% of lightning activities in tropical and subtropical regions. The  
 596 multiple linear regression equations are based on the least-squares method and monthly  
 597 regionally averaged data. Since there is little or no lightning activity in winter, January,  
 598 February, and December are excluded. For the plateau region,

$$599 \quad Y = -0.023 + 0.52 \times 10^{-3}x_1 + 0.12 \times 10^{-3}x_2 - 6.01 \times 10^{-7}x_3 - 2.13 \times$$

$$600 \quad 10^{-5}x_4 - 0.62x_5 - 0.14x_6 + 0.06x_7, \quad (6)$$

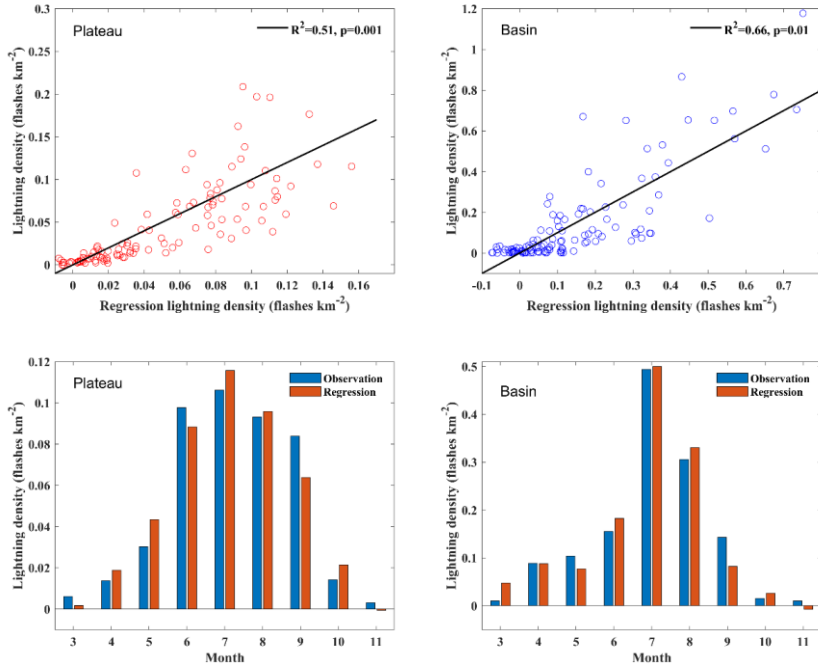
601 and for the basin region,

$$602 \quad Y = -0.29 + 0.49 \times 10^{-3}x_1 - 0.25 \times 10^{-2}x_2 - 0.77 \times 10^{-2}x_3 - 1.53 \times 10^{-5}x_4 +$$

$$603 \quad 10.13x_5 + 0.19x_6 + 0.54x_7, \quad (7)$$

604 where  $Y$  is the CG lightning density,  $x_1$  is CAPE,  $x_2$  is RH,  $x_3$  is SHEAR,  $x_4$  is CBH,  $x_5$   
 605 is TCIW,  $x_6$  is TCLW, and  $x_7$  is sulfate AOD.

606 Figure 122 shows scatter plots and monthly distributions of CG lightning densities  
 607 from multiple linear regression and observations in the plateau and basin regions. The  
 608 scatter plots show that the modeled lightning density tends to be lower than the  
 609 observed lightning density. The correlation in the basin region ( $R^2 = 0.66$ ) is higher than  
 610 that in the plateau region ( $R^2 = 0.51$ ), but both are lower than the correlation reported  
 611 by Stolz et al. (2017). Note that Stolz et al. (2017) examined total lightning on a global  
 612 scale while this study focuses on CG lightning formed over a region with complex  
 613 terrain. The monthly distributions of observed and modeled CG lightning densities in  
 614 the plateau and basin regions show that multiple linear regression can reproduce the  
 615 seasonal variations in lightning activity well. Overall, the best agreement in both  
 616 regions is seen in summer. The best agreements in the plateau and basin regions are  
 617 seen in August and July, respectively.



618 **Figure 122.** Scatter plots of observed CG lightning densities as a function of lightning  
 619 densities from multiple linear regression in the plateau and basin regions (top panels)  
 620 and their monthly distributions (bottom panels).

621

622 To further discuss the main impact factors that contribute to lightning, we use the  
 623 stepwise regression method to select the top three impact factors. The stepwise  
 624 regression equations based on the top three impact factors are as follows:

625 for the plateau region,

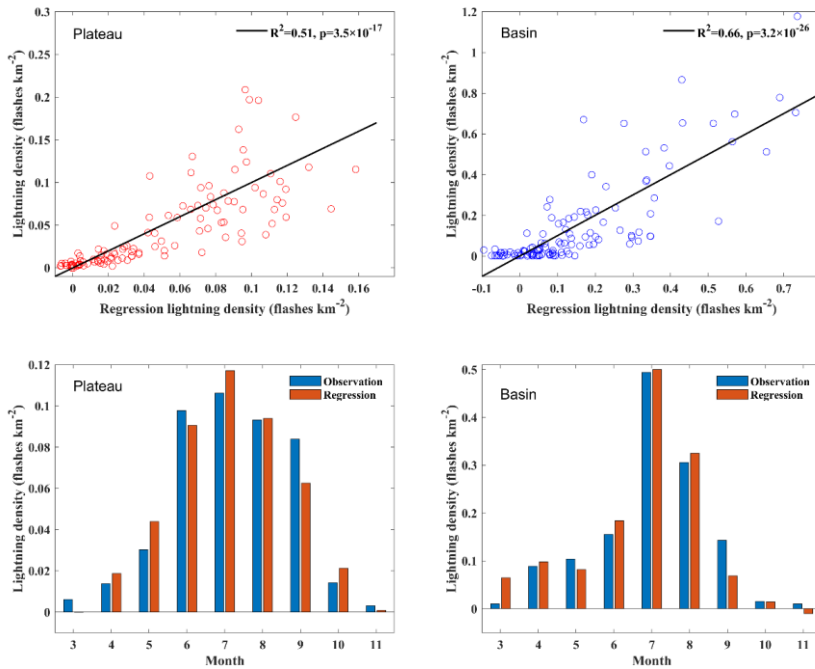
$$626 \quad Y = -0.011 + 0.52 \times 10^{-3}x_1 + 0.25 \times 10^{-3}x_2 - 9.41 \times 10^{-6}x_4, \quad (8)$$

627 and for the basin region,

$$628 \quad Y = -0.48 + 0.55 \times 10^{-3}x_1 + 9.35x_5 + 0.53x_7, \quad (9)$$

629 where  $Y$  is the CG lightning density,  $x_1$  is CAPE,  $x_2$  is RH,  $x_4$  is CBH,  $x_5$  is TCIW, and  
 630  $x_7$  is sulfate AOD. The top three factors contributing to lightning in the plateau region  
 631 are CAPE, RH, and CBH, and the top three factors contributing to lightning in the basin  
 632 region are CAPE, TCIW, and AOD, suggesting that aerosols have a more prominent  
 633 effect on lightning in the basin region.

634 Figure 133 shows scatter plots and monthly distributions of CG lightning densities  
 635 from stepwise regression and observations in the plateau and basin regions. As seen in  
 636 Fig. 122, the modeled lightning density tends to be lower than the observed lightning  
 637 density, with  $R^2$  values of 0.51 and 0.66 in the plateau and basin regions, respectively.  
 638 This also suggests that lightning activity can be reasonably modeled as long as factors  
 639 that contribute significantly to lightning, such as CAPE, are properly determined. The  
 640 monthly distributions of lightning densities modeled by stepwise regression agree with  
 641 observations from March to October reasonably well.



642 **Figure 133.** Scatter plots of observed CG lightning densities as a function of lightning  
 643 densities from stepwise regression in the plateau and basin regions (top panels) and  
 644 their monthly distributions (bottom panels).

645

#### 646 4 Conclusions

647

648 In this study, we investigated the influences of aerosol, thermodynamic, and cloud-  
 649 related factors on CG lightning activity in the plateau and basin regions of Sichuan

650 province, a part of China with complex terrain. Data used to discuss the dependence of  
651 the effect of aerosols on CG lightning on thermodynamic and cloud-related conditions  
652 included the CG lightning density, sulfate AOD, CAPE, RH, SHEAR, CBH, TCLW,  
653 and TCIW from 2005–2017.

654 CG lightning activity over the basin region was much more vigorous than that over  
655 the plateau region, ~~mainly because the CAPE in the basin area was significantly larger~~  
656 ~~than that in the plateau region (Qie et al., 2003) related to the thermodynamic difference~~  
657 ~~between the two regions~~. AODs in the basin region were also significantly higher than  
658 those in the plateau region, mainly due to the large amounts of anthropogenic air  
659 pollutant emissions and the mountainous terrain around the basin area that is not  
660 conducive to the ~~diffusion–dispersion~~ of air pollutants. CG lightning activity was  
661 positively correlated with AOD in the plateau region, but negatively correlated with  
662 AOD in the basin region. The correlation between sulfate AOD and lightning was  
663 stronger than that between total AOD and lightning, and since sulfate AOD accounted  
664 for a high proportion of the total AOD, this study focused on the role of sulfate AOD.  
665 The lightning density over the plateau region increased exponentially with increasing  
666 AOD, while the lightning density over the basin region decreased exponentially with  
667 increasing AOD.

668 CAPE, RH, and TCIW were significantly positively correlated with lightning  
669 activity, while SHEAR was negatively correlated with lightning, suggesting that  
670 convective uplift and ice-phase particles are essential factors for lightning activity. CBH  
671 indirectly represents the warm-cloud thickness and is negatively correlated with TCLW.  
672 The increase in TCLW in the plateau region is beneficial to lightning activity, but not  
673 in the basin region, which may be related to the difference in warm-cloud depths  
674 between the two regions. In the plateau region, because of the compression effect of the  
675 plateau topography on clouds, warm clouds are very thin, and the high liquid water  
676 content is conducive to conveying more supercooled water to the freezing level,  
677 promoting the development of ice-phase clouds and lightning activity. In the basin  
678 region, higher liquid water contents mean robust warm-cloud processes, which are more

679 conducive to the formation of warm rain than ice-phase processes, thus inhibiting  
680 lightning activity. Partial correlation analyses indicate that CAPE, SHEAR, and TCIW  
681 are important factors controlling lightning activity, especially CAPE.

682 To reveal the joint effects of aerosol, thermodynamic, and cloud-related factors on  
683 CG lightning, AOD, CAPE, SHEAR, TCLW, TCIW were selected for further analysis.  
684 In the plateau region, the aerosol loading is relatively low, stimulating lightning activity  
685 through the microphysical effect. An increase in aerosol loading reduces the size of  
686 cloud droplets, generating more but smaller cloud droplets, thus reducing the collision-  
687 coalescence efficiency and inhibiting the warm-rain process. An increase in the liquid  
688 water content of a cloud is conducive to the development of the ice-phase process,  
689 which releases more latent heat and further stimulates convection. The increased  
690 convection and the increase in ice particles lead to more intense lightning activity. In  
691 the basin region, the aerosol loading is very high, which inhibits lightning activity  
692 through the radiative effect. High concentrations of aerosols reduce the solar radiation  
693 reaching the surface through absorption and scattering and reduce the convective  
694 energy from the ground to the lower atmosphere. The weakening of the convective  
695 uplift is not conducive to the transportation of liquid water above the freezing level and  
696 inhibits the development of the ice-phase process. The weakening of convection and  
697 the ice-phase process thus inhibits the intensity of lightning activity. The correlation  
698 between  $RL_m$  and AOD and the correlation between  $RL_r$  and AOD further the idea that  
699 aerosols over the plateau region affect the hydrometeor content in the atmosphere  
700 through the microphysical effect, while aerosols over the basin region mainly affect  
701 convective energy through the radiative effect, both of which affect lightning activity  
702 differently.

703 Our current study is limited to discussing the effect of aerosols on C-G lightning  
704 density. Previous studies have suggested that aerosols affect the intensity and polarity  
705 of C-G lightning (Lyons et al., 1998; Naccarato et al., 2003; Carey et al., 2007; Pawar  
706 et al., 2017). Future studies involving observational data analyses and numerical  
707 simulations will investigate the mechanism by which aerosols affect the C-G lightning

708 polarity by modulating the charge structure.

709

710 *Data availability.* The CG lightning data can be obtained by contacting the first author  
711 (zpg@cuit.edu.cn). MERRA-2 aerosol data can be download from  
712 <https://disc.sci.gsfc.nasa.gov/MERRA/> (last access: 9 September 2019), ~~and~~ the ERA5  
713 data are from <https://cds.climate.copernicus.eu/> (last access: 9 September 2019), the  
714 MISR aerosol data are form <https://eosweb.larc.nasa.gov/> (last access: 3 August 2020),  
715 and the CLARA-A2 data are from  
716 [https://wui.cmsaf.eu/safira/action/viewDoiDetails?acronym=CLARA\\_AVHRR\\_V002](https://wui.cmsaf.eu/safira/action/viewDoiDetails?acronym=CLARA_AVHRR_V002)  
717 (last access: 1 August 2020).

718

719 *Author contributions.* PZ and ZL designed the research ideas for this study; PZ carried  
720 it out and prepared the manuscript; HX, Y. Zheng, FW, XJ, and Y. Zhou provided the  
721 analysis ideas of meteorological and cloud-related parameters. MC edited the  
722 manuscript.

723

724 *Competing interests.* The authors declare that they have no conflict of interest.

725

726 *Acknowledgments.* This research was jointly supported by the National Natural Science  
727 Foundation of China (41905126, 41875169, 41705120), the National Key Research and  
728 Development Project (2018YFC1505702), and the Key Laboratory for Cloud Physics  
729 of China Meteorological Administration LCP/CMA (2017Z016). Pengguo Zhao  
730 acknowledges China Scholarship Council for support (201808515075).

731

## 732 **References**

733 Allen, D. J., and Pickering, K. E.: Evaluating lightning flash rate parameterizations for  
734 use in a global chemical transport model, *J. Geophys. Res. Atmos.*, 107(D23), 4711,  
735 <https://doi.org/10.1029/2002JD002066>, 2002.

736 Altaratz, O., Koren, I., Yair, Y., and Price, C.: Lightning response to smoke from

域代码已更改

737 Amazonian fires, *Geophys. Res. Lett.*, 37, L07801,  
738 <https://doi.org/10.1029/2010GL042679>, 2010.

739 Altaratz, O., Kucienska, B., Kostinski, A., Raga, G. B., and Koren, I.: Global  
740 association of aerosol with flash density of intense lightning, *Environ. Res. Lett.*,  
741 12, 114037, <https://doi.org/10.1088/1748-9326/aa922b>, 2017.

742 Bang, S. D., and Zipser E. J.: Seeking reasons for the differences in size spectra of  
743 electrified storms over land and ocean, *J. Geophys. Res. Atmos.*, 121, 9048–9068,  
744 <https://doi.org/10.1002/2016JD025150>, 2016.

745 Buchard, V., Randles, C.A., Da Silva, A.M., Darmenov, A., Colarco, P.R., Govindaraju,  
746 R., Ferrare, R., Hair, J., Beyersdorf, A.J., Ziemba, L.D. and Yu, H.: The MERRA-2  
747 aerosol reanalysis, 1980 onward. Part II: Evaluation and case studies, *J. Climate*,  
748 30(17), 6851–6872, <https://doi.org/10.1175/JCLI-D-16-0613.1>, 2017.

749 Carey, L. D., and Buffalo, K. M.: Environmental control of cloud-to-ground lightning  
750 polarity in severe storms, *Mon. weather rev.*, 135(4), 1327–1353,  
751 <https://doi.org/10.1175/MWR3361.1>, 2007.

752 Carrió, G. G., and Cotton, W. R.: On the buffering of CCN impacts on wintertime  
753 orographic clouds: An idealized examination, *Atmos. Res.*, 137, 136–144,  
754 <https://doi.org/10.1016/j.atmosres.2013.09.011>, 2014.

755 China Meteorological Administration, 2009: China Lightning Monitoring Reports (in  
756 Chinese). China Meteorological Press, 142 pp., 2008.

757 Cummins, K. L., and Murphy, M. J., Bardo, E. A., Hiscox, W. L., Pyle, R. B., and Pifer,  
758 A. E.: A combined TOA/MDF technology upgrade of the U.S. National Lightning  
759 Detection Network, *J. Geophys. Res. Atmos.*, 103, 9035–9044,  
760 <https://doi.org/10.1029/98JD00153>, 1998.

761 Cummins, K. L., and M. J. Murphy: An overview of lightning locating systems: History,  
762 techniques, and data uses, with an in-depth look at the U.S. NLDN. *IEEE Trans.*  
763 *Electromagn. Compat.*, 51, 499–518, <https://doi.org/10.1109/TEM.2009.2023450>,  
764 2009.

765 Dafis, S., Fierro, A., Giannaros, T. M., Kotroni, V., Lagouvardos, K. and Mansell, E.,

766 Performance evaluation of an explicit lightning forecasting system. *J. Geophys. Res.*  
767 *Atmos.*, 123(10), 5130–5148, <https://doi.org/10.1029/2017JD027930>, 2018.

768 Dee, D. P., and Coauthors: The ERA-Interim reanalysis: Configuration and  
769 performance of the data assimilation system. *Q. J. R. Meteorolog. Soc.*, 137(656),  
770 553–597, <https://doi.org/10.1002/qj.828>, 2011.

771 Davies-Jones, R.: Linear and nonlinear propagation of supercell storms, *J. Atmos. Sci.*,  
772 59, 3178–3205,  
773 [https://doi.org/10.1175/15200469\(2003\)059<3178:LANPOS>2.0.CO;2](https://doi.org/10.1175/15200469(2003)059<3178:LANPOS>2.0.CO;2), 2002.

774 Fan, J., Yuan, T., Comstock, J. M., Ghan, S., Khain, A., Leung, L. R., Li, Z., Martins,  
775 V. J. and Ovchinnikov, M.: Dominant role by vertical wind shear in regulating  
776 aerosol effects on deep convective clouds. *J. Geophys. Res. Atmos.*, 114(D22),  
777 <https://doi.org/10.1029/2009JD012352>, 2009.

778 Fan, J., Rosenfeld, D., Yang, Y., Zhao, C., Leung, L. R. and Li, Z.: Substantial  
779 contribution of anthropogenic air pollution to catastrophic floods in Southwest  
780 China. *Geophys. Res. Lett.*, 42(14), 6066-6075,  
781 <https://doi.org/10.1002/2015GL064479>, 2015.

782 Fan, J., Rosenfeld, D., Zhang, Y., Giangrande, S., Li, Z., Machado, L., et al. Substantial  
783 convection and precipitation enhancements by ultrafine aerosol particles. *Science*,  
784 359(6374), 411–418. <https://doi.org/10.1126/science.aan8461>, 2018.

785 Freychet, N., Tett, S. F. B., Yan, Z., and Li, Z.: Underestimated change of wet-bulb  
786 temperatures over East and South China, *Geophys. Res. Lett.*, 47, e2019GL086140,  
787 <https://doi.org/10.1029/2019GL086140>, 2020.

788 Fuchs, B. R., Rutledge, S. A., Bruning, E. C., Pierce, J. R., Kodros, J. K., Lang, T. J.,  
789 MacGorman, D. R., Krehbiel, P. R., and Rison, W.: Environmental controls on  
790 storm intensity and charge structure in multiple regions of the continental United  
791 States, *J. Geophys. Res. Atmos.*, 120, 6575–6596,  
792 <https://doi.org/10.1002/2015JD023271>, 2015.

793 Guo, J., Deng, M., Lee, S.S., Wang, F., Li, Z., Zhai, P., Liu, H., Lv, W., Yao, W. and Li,  
794 X.: Delaying precipitation and lightning by air pollution over the Pearl River Delta.



795 Part I: Observational analyses, *J. Geophys. Res. Atmos.*, 121, 6472–6488,  
796 <https://doi.org/10.1002/2015JD023257>, 2016.

797 Hoffmann, L., Günther, G., Li, D., Stein, O., Wu, X., Griessbach, S., Heng, Y., Konopka,  
798 P., Müller, R., Vogel, B. and Wright, J. S.: From ERA-Interim to ERA5: the  
799 considerable impact of ECMWF’s next-generation reanalysis on Lagrangian  
800 transport simulations, *Atmos. Chem. Phys.*, 19, 3097–3124,  
801 <https://doi.org/10.5194/acp-19-3097-2019>, 2019.

802 Huang, J., Zhang, C., and Prospero, J. M.: Large-scale effect of aerosols on precipitation  
803 in the West African Monsoon region, *Q. J. R. Meteorolog. Soc.*, 135 581–94,  
804 <https://doi.org/10.1002/qj.391>, 2009.

805 Jiang, J. H., Su, H., Huang, L., Wang, Y., Massie, S., Zhao, B., Omar A, Wang, Z.:  
806 Contrasting effects on deep convective clouds by different types of aerosols. *Nat.*  
807 *commun.*, 9(1), 1–7, <https://doi.org/10.1038/s41467-018-06280-4>, 2018.

808 Kar, S. K., Liou, Y. A., and Ha, K. J.: Aerosol effects on the enhancement of cloud-to-  
809 ground lightning over major urban areas of South Korea, *Atmos. Res.*, 92, 80-87,  
810 <https://doi.org/10.1016/j.atmosres.2008.09.004>, 2009.

811 Kar, S. K., and Liou, Y. A.: Enhancement of cloud-to-ground lightning activity over  
812 Taipei, Taiwan in relation to urbanization, *Atmos. Res.*, 147–148, 111–120,  
813 <https://doi.org/10.1016/j.atmosres.2014.05.017>, 2014.

814 [Karlsson, K. G., Anttila, K., Trentmann, J., Stengel, M., Meirink, J. F., Devasthale, A.:](#)  
815 [CLARA-A2: the second edition of the CM SAF cloud and radiation data record](#)  
816 [from 34 years of global AVHRR data. \*Atmos. Chem. Phys.\*, 17, 5809–5828.](#)  
817 [<https://doi.org/10.5194/acp-17-5809-2017>](#), 2017.

818 [Karlsson, K. G. and Håkansson, N.: Characterization of AVHRR global cloud detection](#)  
819 [sensitivity. \*Atmos. Chem. Phys.\*, 11, 633–649. \[https://doi.org/10.5194/amt-11-633-\]\(https://doi.org/10.5194/amt-11-633-2018\)](#)  
820 [2018, 2018.](#)

821 Khain, A., Cohen, N., Lynn, B., Pokrovsky, A.: Possible aerosol effects on lightning  
822 activity and structure of hurricanes, *J. Atmos. Sci.*, 65, 3652–3667,  
823 <https://doi.org/10.1175/2008JAS2678.1>, 2008.

824 Koren, I., Martins, J. V., Remer, L. A. and Afargan, H.: Smoke invigoration versus  
825 inhibition of clouds over the Amazon, *Science*, 321, 946–949,  
826 <https://doi.org/10.1126/science.1159185>, 2008.

827 Koren, I., Altaratz, O., Remer, L. A., Feingold, G., Martins, J. V., and Heiblum, R. H.:  
828 Aerosol-induced intensification of rain from the tropics to the mid-latitudes, *Nat.*  
829 *Geosci.*, 5, 118–122, <https://doi.org/10.1038/ngeo1364>, 2012.

830 Koren, I., Dagan, G., and Altaratz, O.: From aerosol-limited to invigoration of warm  
831 convective clouds, *Science*, 344, 1143–1146,  
832 <https://doi.org/10.1126/science.1252595>, 2014.

833 Lee, S. S., Guo, J., and Li, Z.: Delaying precipitation by air pollution over the Pearl  
834 River Delta: 2. Model simulations, *J. Geophys. Res. Atmos.*, 121, 11739–11760,  
835 [doi:10.1002/2015JD024362](https://doi.org/10.1002/2015JD024362), 2016.

836 Lee, S., Hwang, S. O., Kim, J. and Ahn, M. H.: Characteristics of cloud occurrence  
837 using ceilometer measurements and its relationship to precipitation over Seoul,  
838 *Atmos. Res.*, 201, 46–57, <https://doi.org/10.1016/j.atmosres.2017.10.010>, 2018.

839 Lei, Y., Letu, H., Shang, H., and Shi, J.: Cloud cover over the Tibetan Plateau and  
840 eastern China: a comparison of ERA5 and ERA-Interim with satellite observations,  
841 *Clim. Dynam.*, 1–17, <https://doi.org/10.1007/s00382-020-05149-x>, 2020.

842 Li, Z., Niu, F., Fan, J., Liu, Y., Rosenfeld, D. and Ding, Y.: Long-term impacts of  
843 aerosols on the vertical development of clouds and precipitation, *Nat. Geosci.*, 4(12),  
844 888–894, <https://doi.org/10.1038/ngeo1313>, 2011.

845 Li, Z., Rosenfeld, D., Fan, J.: Aerosols and their impact on radiation, clouds,  
846 precipitation, and severe weather events, *Oxford Research Encyclopedias*, PNNL-  
847 SA-124900, <https://doi.org/10.1093/acrefore/9780199389414.013.126>, 2017.

848 Li, Z., Wang, Y., Guo, J., Zhao, C., Cribb, M. C., Dong, X., Fan, J., Gong, D., Huang,  
849 J., Jiang, M. and Jiang, Y., et al.: East Asian Study of Tropospheric Aerosols and  
850 their Impact on Regional Clouds, Precipitation, and Climate (EAST-AIR<sub>CPC</sub>), *J.*  
851 *Geophys. Res. Atmos.*, 124, <https://doi.org/10.1029/2019JD030758>, 2019, 2019.

852 [Li, X., Guo, X. and Fu, D.: TRMM-retrieved cloud structure and evolution of MCSs](#)

853 [over the northern South China Sea and impacts of CAPE and vertical wind shear.](#)  
854 [Adv. Atmos. Sci. 30, 77–88, <https://doi.org/10.1007/s00376-012-2055-2>, 2013.](#)

855 Li, X., Pan, Y., and Mo, Z.: Joint effects of several factors on cloud-to-ground lightning  
856 and rainfall in Nanning (China), *Atmos. Res.*, 212, 23–32,  
857 <https://doi.org/10.1016/j.atmosres.2018.05.002>, 2018.

858 [Liu, H., Guo, J., Koren, I., Altaratz, O., Dagan, G., Wang, Y., Jiang, J.H., Zhai, P. and](#)  
859 [Yung, Y.L.: Non-monotonic aerosol effect on precipitation in convective clouds](#)  
860 [over tropical oceans. Sci. Rep., 9\(1\), 1–7, \[https://doi.org/10.1038/s41598-019-\]\(https://doi.org/10.1038/s41598-019-44284-2\)](#)  
861 [44284-2, 2019.](#)

862 Lyons, W. A., Nelson, T. E., Williams, E. R., Cramer, J. A., and Turner, T. R.: Enhanced  
863 positive cloud-to-ground lightning in thunderstorms ingesting smoke from fires,  
864 *Science*, 282(5386), 77–80, <https://doi.org/10.1126/science.282.5386.77>, 1998.

865 MacGorman, D. R., Straka, J. M., Ziegler, C. L.: A lightning parameterization for  
866 numerical cloud models, *J. Appl. Meteorol.*, 40, 459–478,  
867 [https://doi.org/10.1175/1520-0450\(2001\)040<0459:ALPFNC>2.0.CO;2](https://doi.org/10.1175/1520-0450(2001)040<0459:ALPFNC>2.0.CO;2), 2001.

868 Mansell, E. R., MacGorman, D. R., Ziegler, C. L., Straka, J. M.: Charge structure and  
869 lightning sensitivity in a simulated multicell thunderstorm, *J. Geophys. Res. Atmos.*,  
870 110(D12): 1545–1555, <https://doi.org/10.1029/2004JD005287>, 2005.

871 Mansell, E. R., Ziegler, C. L.: Aerosol Effects on Simulated Storm Electrification and  
872 Precipitation in a Two-Moment Bulk Microphysics Model, *J. Atmos. Sci.*, 70,  
873 2032–2050, <https://doi.org/10.1175/JAS-D-12-0264.1>, 2013.

874 Minzner, R. A.: The 1976 standard atmosphere and its relationship to earlier standards.  
875 *Rev. geophys.*, 15(3), 375–384, <https://doi.org/10.1029/RG015i003p00375>, 1977.

876 Naccarato, K. P., Pinto Jr, O., and Pinto, I. R. C. A.: Evidence of thermal and aerosol  
877 effects on the cloud-to-ground lightning density and polarity over large urban areas  
878 of Southeastern Brazil, *Geophys. Res. Lett.*, 30(13),  
879 <https://doi.org/10.1029/2003GL017496>, 2003.

880 [Ning, G., Wang, S., Ma, M., Ni, C., Shang, Z., Wang, J. and Li, J.: Characteristics of](#)  
881 [air pollution in different zones of Sichuan Basin, China. Sci. Total Environ., 612,](#)

882 [975–984, https://doi.org/10.1016/j.scitotenv.2017.08.205](https://doi.org/10.1016/j.scitotenv.2017.08.205), 2018a.

883 Ning, G., Wang, S., Yim, S., Li, J., Hu, Y., Shang, Z., Wang, J. and Wang, J.: Impact of  
884 low-pressure systems on winter heavy air pollution in the northwest Sichuan Basin,  
885 China, *Atmos. Chem. Phys.*, 18(18), 13601–13615, [https://doi.org/10.5194/acp-18-](https://doi.org/10.5194/acp-18-13601-2018)  
886 [13601-2018](https://doi.org/10.5194/acp-18-13601-2018), 2018b.

887 [Ning, G., Yim, S.H.L., Wang, S., Duan, B., Nie, C., Yang, X., Wang, J. and Shang, K.:  
888 \*Synergistic effects of synoptic weather patterns and topography on air quality: a  
889 case of the Sichuan Basin of China, Clim. Dynam.\*, 53\(11\), 6729–6744,  
890 <https://doi.org/10.1007/s00382-019-04954-3>, 2019.](https://doi.org/10.1007/s00382-019-04954-3)

891 Oreopoulos, L., Cho, N., and Lee, D.: A global survey of apparent aerosol-cloud  
892 interaction signals, *J. Geophys. Res.*, 125, e2019JD031287,  
893 <https://doi.org/10.1029/2019JD031287>, 2020.

894 Orville, R. E., Huffines, G. R., Burrows, W. R., and Cummins, K. L.: The North  
895 American lightning detection network (NALDN)-Analysis of flash data: 2001–09,  
896 *Mon. Weather Rev.*, 139(5), 1305–1322, <https://doi.org/10.1175/2010MWR3452.1>,  
897 2011.

898 Pawar, S. D., Gopalakrishnan, V., Murugavel, P., Veremey, N. E. and Sinkevich, A. A.:  
899 Possible role of aerosols in the charge structure of isolated thunderstorms. *Atmos.*  
900 *Res.*, 183, 331–340, <https://doi.org/10.1016/j.atmosres.2016.09.016>, 2017.

901 Pinto, I. R. C. A., Pinto, Jr O., Gomes, M. A. S. S., Ferreira, N. J.: Urban effect on the  
902 characteristics of cloud-to-ground lightning over Belo Horizonte-Brazil, *Ann.*  
903 *Geophys.*, 22, 697–700, 2004.

904 Price, C. G.: Lightning Applications in Weather and Climate Research, *Surv. Geophys.*,  
905 34, 755–767. <https://doi.org/10.1007/s10712-012-9218-7>, 2013.

906 Proestakis, E., Kazadzis, S., Lagouvardos, K., Kotroni, V., and Kazantzidis, A.:  
907 Lightning activity and aerosols in the Mediterranean region, *Atmos. Res.*, 170, 66–  
908 75, <https://doi.org/10.1016/j.atmosres.2015.11.010>, 2016.

909 Qian, Y., Gong, D., Fan, J., Leung, L. R., Bennartz, R., Chen, D., and Wang, W.: Heavy  
910 pollution suppresses light rain in China: Observations and modeling. *J. Geophys.*

911 Res. Atmos., 114(D7), <https://doi.org/10.1029/2008JD011575>, 2009.

912 [Qie, X., Toumi, R., Zhou, Y. J.: Lightning activity on the central Tibetan Plateau and its](#)  
913 [response to convective available potential energy, Chinese Science Bulletin, 48\(3\),](#)  
914 [296–299, https://doi.org/10.1007/BF03183302, 2003.](#)

915 Qie, X., and Zhang, Y.: A Review of Atmospheric Electricity Research in China from  
916 2011 to 2018, *Adv. Atmos. Sci.*, 36, 994–1014, [https://doi.org/10.1007/s00376-019-](https://doi.org/10.1007/s00376-019-8195-x)  
917 [8195-x](#), 2019.

918 Ramos, A. M., R. Ramos, P. Sousa, R. M. Trigo, M. Janeira, and Prior, V.: Cloud to  
919 ground lightning activity over Portugal and its association with circulation weather  
920 types, *Atmos. Res.*, 101, 84–101, <https://doi.org/10.1016/j.atmosres.2011.01.014>,  
921 2011.

922 Randles, C. A., Da Silva, A. M., Buchard, V., Colarco, P. R., Darmenov, A., Govindaraju,  
923 R., Smirnov, A., Holben, B., Ferrare, R., Hair, J. and Shinozuka, Y.: The MERRA-  
924 2 aerosol reanalysis, 1980 onward. Part I: System description and data assimilation  
925 evaluation. *J. Climate*, 30(17), 6823-6850, [https://doi.org/10.1175/JCLI-D-16-](https://doi.org/10.1175/JCLI-D-16-0609.1)  
926 [0609.1](#), 2017.

927 Romps, D. M., Seeley, J. T., Vollaro, D. and Molinari, J.: Projected increase in lightning  
928 strikes in the United States due to global warming, *Science*, 346(6211), 851-854,  
929 <https://doi.org/10.1126/science.1259100>, 2014.

930 Romps, D. M., Charn, A. B., Holzworth, R. H., Lawrence, W. E., Molinari, J., and  
931 Vollaro, D.: CAPE times P explains lightning over land but not the land-ocean  
932 contrast. *Geophys. Res. Lett.*, 45, 12, 623–12, 630,  
933 <https://doi.org/10.1029/2018GL080267>, 2018.

934 Rosenfeld, D., Dai, J., Yu, X., Yao, Z., Xu, X., Yang, X., and Du, C.: Inverse relations  
935 between amounts of air pollution and orographic precipitation, *Science*, 315: 1396-  
936 1398, <https://doi.org/10.1126/science.1137949>, 2007.

937 Rosenfeld, D., Lohmann, U., Raga, G. B., O'Dowd, C. D., Kulmala, M., Fuzzi, S.,  
938 Reissell, A. and Andreae, M. O.: Flood or Drought: How Do Aerosols Affect  
939 Precipitation, *Science*, 321: 1309-1313, <https://doi.org/10.1126/science.1160606>,

940 2008.

941 Saunders, C.: Charge separation mechanisms in clouds, *Space Sci. Rev.*, 137, 335–53,  
942 <https://doi.org/10.1007/s11214-008-9345-0>, 2008.

943 Saunders, C. P. R., Keith, W. D., and Mitzeva. R. P.: The effect of liquid water on  
944 thunderstorm charging, *J. Geophys. Res. Atmos.*, 96, 11007–17,  
945 <https://doi.org/10.1029/91JD00970>, 1991.

946 [Sherburn, K.D., Parker, M.D., King, J.R. and Lackmann, G.M.: Composite](#)  
947 [environments of severe and nonsevere high-shear, low-CAPE convective events,](#)  
948 [Wea. forecasting, 31\(6\), 1899-1927. <https://doi.org/10.1175/WAF-D-16-0086.1>,](#)  
949 [2016.](#)

950 Shi, Z., Tan, Y., Tang, H., Sun, J., Yang, Y., Peng, L. and Guo, X.: Aerosol effect on the  
951 land-ocean contrast in thunderstorm electrification and lightning frequency. *Atmos.*  
952 *Res.*, 164-165: 131-141, <https://doi.org/10.1016/j.atmosres.2015.05.006>, 2015.

953 Shou, Y., Lu, F., Liu, H., Cui, P., Shou, S., and Liu, J.: Satellite-based observational  
954 study of the Tibetan Plateau Vortex: Features of deep convective cloud tops, *Adv.*  
955 *Atmos. Sci.*, 36(2), 189–205, <https://doi.org/10.1007/s00376-018-8049-y>, 2019.

956 Stallins, J. A., Carpenter, J., Bentley, M. L., Ashley, W. S. and Mulholland, J. A.:  
957 Weekend-weekday aerosols and geographic variability in cloud-to-ground lightning  
958 for the urban region of Atlanta, Georgia, USA. *Reg. Environ. Change*, 13(1), 137–  
959 151, <https://doi.org/10.1007/s10113-012-0327-0>, 2013.

960 Stolz, D. C., Rutledge, S. A., and Pierce, J. R.: Simultaneous influences of  
961 thermodynamics and aerosols on deep convection and lightning in the tropics, *J.*  
962 *Geophys. Res. Atmos.*, 120(12), 6207–6231,  
963 <https://doi.org/10.1002/2014JD023033>, 2015.

964 Stolz, D. C., Rutledge, S. A., Pierce, J. R., and van den Heever, S. C.: A global lightning  
965 parameterization based on statistical relationships among environmental factors,  
966 aerosols, and convective clouds in the TRMM climatology, *J. Geophys. Res. Atmos.*,  
967 122, 7461-7492, <https://doi.org/10.1002/2016JD026220>, 2017.

968 Sun, E., Che, H., Xu, X., Wang, Z., Lu, C., Gui, K., Zhao, H., Zheng, Y., Wang, Y.,

969 Wang, H. and Sun, T.: Variation in MERRA-2 aerosol optical depth over the  
970 Yangtze River Delta from 1980 to 2016, *Theor. Appl. Climatol.*, 136(1-2),  
971 <https://doi.org/10.1007/s00704-018-2490-9>, 363-375, 2019a.

972 Sun, E., Xu, X., Che, H., Tang, Z., Gui, K., An, L., Lu, C., and Shi, G.: Variation in  
973 MERRA-2 aerosol optical depth and absorption aerosol optical depth over China  
974 from 1980 to 2017. *J. Atmos. Sol.-Terr. Phy.*, 186, 8-19,  
975 <https://doi.org/10.1016/j.jastp.2019.01.019>, 2019b.

976 Sun, L., Wei, J., Duan, D. H., Guo, Y. M., Yang, D. X., Jia, C., and Mi, X.: Impact of  
977 Land-Use and Land-Cover Change on urban air quality in representative cities of  
978 China. *J. Atmos. Sol.-Terr. Phy.*, 142, 43-54,  
979 <https://doi.org/10.1016/j.jastp.2016.02.022>, 2016.

980 Tan, Y., Peng, L., Shi, Z. and Chen, H.: Lightning flash density in relation to aerosol  
981 over Nanjing (China), *Atmos. Res.*, 174, 1-8,  
982 <https://doi.org/10.1016/j.atmosres.2016.01.009>, 2016.

983 Thompson, R. L., Mead, C. M., and Edwards, R.: Effective storm-relative helicity and  
984 bulk shear in supercell thunderstorm environments, *Weather Forecast.*, 22, 102–115,  
985 <https://doi.org/10.1175/WAF969.1>, 2007.

986 Thornton, J. A., Virts, K. S., Holzworth, R. H. and Mitchell, T. P.: Lightning  
987 enhancement over major oceanic shipping lanes, *Geophys. Res. Lett.*, 44(17), 9102-  
988 9111, <https://doi.org/10.1002/2017GL074982>, 2017.

989 Tinmaker, M. I. R., Ghude, S. D., Chate, D. M.: Land-sea contrasts for climatic  
990 lightning activity over Indian region, *Theor. Appl. Climatol.*, 138(1-2), 931-940,  
991 <https://doi.org/10.1007/s00704-019-02862-4>, 2019.

992 Tippet, M. K., and Koshak, W. J.: A baseline for the predictability of U.S. cloud-to-  
993 ground lightning. *Geophys. Res. Lett.*, 45, 10719–10728,  
994 <https://doi.org/10.1029/2018GL079750>, 2018.

995 Tippet, M. K., Lepore, C., Koshak, W. J., Chronis, T. and Vant-Hull, B.: Performance  
996 of a simple reanalysis proxy for US cloud-to-ground lightning. *Int. J. Climatol.*,  
997 39(10), 3932-3946, <https://doi.org/10.1002/joc.6049>, 2019.

998 Wall, C., Zipser, E. J., and Liu, C.: An investigation of the aerosol indirect effect on  
999 convective intensity using satellite observations, *J. Atmos. Sci.*, 71, 430–447,  
1000 <https://doi.org/10.1175/JAS-D-13-0158.1>, 2014.

1001 Wang, Y., Wan, Q., Meng, W., Liao, F., Tan, H., and Zhang, R.: Long-term impacts of  
1002 aerosols on precipitation and lightning over the Perl River Delta megacity area in  
1003 China. *Atmos. Chem. Phys.*, 11, 12421–12436, [https://doi.org/10.5194/acp-11-](https://doi.org/10.5194/acp-11-12421-2011)  
1004 [12421-2011](https://doi.org/10.5194/acp-11-12421-2011), 2011.

1005 [Wang, Y., Khalizov, A., Levy, M. and Zhang, R.: New Directions: Light absorbing](#)  
1006 [aerosols and their atmospheric impacts. \*Atmos. Environ.\*, 81, 713–715,](#)  
1007 [<https://doi.org/10.1016/j.atmosenv.2013.09.034>, 2013.](#)

1008 Wang, Q., Li, Z., Guo, J., Zhao, C. and Cribb, M.: The climate impact of aerosols on  
1009 the lightning flash rate: is it detectable from long-term measurements?, *Atmos.*  
1010 *Chem. Phys.*, 18(17), 12797–12816, <https://doi.org/10.5194/acp-18-12797-2018>,  
1011 2018.

1012 Wei, J., Huang, W., Li, Z., Xue, W., Peng, Y., Sun, L., and Cribb, M.: Estimating 1-km-  
1013 resolution PM2.5 concentrations across China using the space-time random forest  
1014 approach, *Remote Sens. Environ.*, 231, 111221,  
1015 <https://doi.org/10.1016/j.rse.2019.111221>, 2019a.

1016 Wei, J., Li, Z., Guo, J., Sun, L., Huang, W., Xue, W., Fan, T., and Cribb, M. Satellite-  
1017 derived 1-km-resolution PM1 concentrations from 2014 to 2018 across China,  
1018 *Environmen. Sci. Technol.*, 53(22), 13265–13274,  
1019 <https://doi.org/10.1021/acs.est.9b03258>, 2019b.

1020 [Wei, J., Peng, Y., Mahmood, R., Sun, L. and Guo, J., 2019. Intercomparison in spatial](#)  
1021 [distributions and temporal trends derived from multi-source satellite aerosol](#)  
1022 [products. \*Atmos. Chem. Phys.\*, 19, 7183–7207, \[https://doi.org/10.5194/acp-19-\]\(https://doi.org/10.5194/acp-19-7183-2019\)](#)  
1023 [\[7183-2019\]\(https://doi.org/10.5194/acp-19-7183-2019\), 2019c.](#)

1024 Westcott, N. E.: Summertime cloud-to-ground lightning activity around major  
1025 Midwestern urban areas, *J. Appl. Meteorol.*, 34: 1633-1642,  
1026 <https://doi.org/10.1175/1520-0450-34.7.1633>, 1995.



1027 Williams, E. R.: Lightning and climate: A review. *Atmos. Res.*, 76, 272-287,  
1028 <https://doi.org/10.1016/j.atmosres.2004.11.014>, 2005.

1029 Williams, E. and Stanfill, S.: The physical origin of the land-ocean contrast in lightning  
1030 activity. *C. R. Phys.*, 3(10), 1277-1292, <https://doi.org/10.1016/S1631->  
1031 [0705\(02\)01407-X](https://doi.org/10.1016/S1631-0705(02)01407-X), 2002.

1032 Williams, E. R., Chan, T., and Boccippio, D.: Islands as miniature continents: another  
1033 look at the land ocean lightning contrast, *J. Geophys. Res. Atmos.*, 109,  
1034 <https://doi.org/10.1029/2003JD003833>, 2004.

1035 Williams, E. R., Mushtak, V., Rosenfeld, D., Goodman, S., and Boccippio, D.:  
1036 Thermodynamic conditions favorable to superlative thunderstorm updraft, mixed  
1037 phase microphysics and lightning flash rate, *Atmos. Res.*, 76, 288–306,  
1038 <https://doi.org/10.1016/j.atmosres.2004.11.009>, 2005.

1039 Wong, J., Barth, M.C. and Noone, D.: Evaluating a lightning parameterization based on  
1040 cloud-top height for mesoscale numerical model simulations, *Geosci. Model Dev.*,  
1041 6(2), 429–443, <https://doi.org/10.5194/gmd-6-429-2013>, 2013.

1042 Xia, R., Zhang, D. L., and Wang, B.: A 6-yr cloud-to-ground lightning climatology and  
1043 its relationship to rainfall over central and eastern China. *J. Appl. Meteorol. Clim.*,  
1044 54(12), 2443–2460, <https://doi.org/10.1175/JAMC-D-15-0029.1>, 2015.

1045 Yair, Y., Lynn, B., Price, C., Kotroni, V., Lagouvardos, K., Morin, E., Mugnai, A. and  
1046 Llasat, M. D. C.: Predicting the potential for lightning activity in Mediterranean  
1047 storms based on the Weather Research and Forecasting (WRF) model dynamic and  
1048 microphysical fields. *J. Geophys. Res. Atmos.*, 115(D4),  
1049 <http://dx.doi.org/10.1029/2008JD010868>, 2010.

1050 Yair, Y. Lightning hazards to human societies in a changing climate. *Environ. Res. Lett.*,  
1051 13(12), 123002, <http://dx.doi.org/10.1088/1748-9326/aaea86>, 2018.

1052 Yang, X., Yao, Z., Li, Z. and Fan, T.: Heavy air pollution suppresses summer  
1053 thunderstorms in central China. *J. Atmos. Sol.-Terr. Phy.*, 95,  
1054 <https://doi.org/10.1016/j.jastp.2012.12.023>, 28–40, 2013.

1055 Yang, X., and Li, Z.: Increases in thunderstorm activity and relationships with air

1056 pollution in southeast China, *J. Geophys. Res. Atmos.*, 119, 1835–1844,  
1057 <https://doi.org/10.1002/2013JD021224>, 2014.

1058 Yang, X., Li, Z., Liu, L., Zhou, L., Cribb, M., and Zhang, F.: Distinct weekly cycles of  
1059 thunderstorms and a potential connection with aerosol type in China, *Geophys. Res.*  
1060 *Let.*, 43, 8760–8768, [10.1002/2016GL070375](https://doi.org/10.1002/2016GL070375), 2016.

1061 Yang, X., Sun, J., and Li, W.: An analysis of cloud-to-ground lightning in China during  
1062 2010–13, *Weather Forecast.*, 30(6), 1537–1550, [https://doi.org/10.1175/WAF-D-](https://doi.org/10.1175/WAF-D-14-00132.1)  
1063 [14-00132.1](https://doi.org/10.1175/WAF-D-14-00132.1), 2015.

1064 Yu, R., Xu, Y., Zhou, T., and Li, J.: Relation between rainfall duration and diurnal  
1065 variation in the warm season precipitation over central eastern China, *Geophys. Res.*  
1066 *Let.*, 34, L13703, <https://doi.org/10.1029/2006GL028129>, 2007.

1067 Yuan, T., Remer, L. A., Pickering, K. E., Yun, H.: Observational evidence of aerosol  
1068 enhancement of lightning activity and convective invigoration, *Geophys. Res. Let.*,  
1069 38, L04701, <https://doi.org/10.1029/2010GL046052>, 2011.

1070 Zhang, X., Wang, Y., Niu, T., Zhang, X., Gong, S., Zhang, Y., and Sun, J.: Atmospheric  
1071 aerosol compositions in China: spatial/temporal variability, chemical signature,  
1072 regional haze distribution and comparisons with global aerosols. *Atmos. Chem.*  
1073 *Phys.*, 12: 779–799, <https://doi.org/10.5194/acp-12-779-2012>, 2012.

1074 Zhang, Y., Sun, J. and Fu, S.: Impacts of diurnal variation of mountain-plain solenoid  
1075 circulations on precipitation and vortices east of the Tibetan Plateau during the mei-  
1076 yu season, *Adv. Atmos. Sci.*, 31, 139–153, [https://doi.org/10.1007/s00376-013-](https://doi.org/10.1007/s00376-013-2052-0)  
1077 [2052-0](https://doi.org/10.1007/s00376-013-2052-0), 2014.

1078 Zhang, Y., Cai, C., Chen, B. and Dai, W.: Consistency evaluation of precipitable water  
1079 vapor derived from ERA5, ERA-Interim, GNSS, and radiosondes over China.  
1080 *Radio Sci.*, 54(7), 561–571, <https://doi.org/10.1029/2018RS006789>, 2019.

1081 [Zhao, B., Wang, Y., Gu, Y., Liou, K.N., Jiang, J.H., Fan, J., Liu, X., Lei, H., Yung, Y.L.:  
1082 Ice nucleation by aerosols from anthropogenic pollution. \*Nat. Geosci.\*, 12, 602–607,  
1083 <https://doi.org/10.1038/s41561-019-0389-4>, 2019.](https://doi.org/10.1038/s41561-019-0389-4)

1084 Zhao, C., Tie, X. and Lin, Y.: A possible positive feedback of reduction of precipitation

1085 and increase in aerosols over eastern central China, *Geophys. Res. Lett.*, 33, L11814,  
1086 <https://doi.org/10.1029/2006GL025959>, 2006.

1087 Zhao, C., Lin, Y., Wu, F., Wang, Y., Li, Z., Rosenfeld, D., and Wang, Y.: Enlarging  
1088 rainfall area of tropical cyclones by atmospheric aerosols, *Geophys. Res. Lett.*, 45,  
1089 8604–8611, <https://doi.org/10.1029/2018GL079427>, 2018.

1090 Zhao, P., Yin, Y. and Xiao, H.: The effects of aerosol on development of thunderstorm  
1091 electrification: A numerical study, *Atmos. Res.*, 153, 376–391,  
1092 <https://doi.org/10.1016/j.atmosres.2014.09.011>, 2015.